2016

Molecularly Imprinted Polymers for Enantiomer Separations and Biomolecular Sensors

Britney Lyn Hebert
Louisiana State University and Agricultural and Mechanical College, bhebe58@lsu.edu

MOLECULARY IMPRINTED POLYMERS FOR ENANTIOMER SEPARATIONS AND BIOMELCULAR SENSORS

A Dissertation

Submitted to the Graduate Faculty of the
Louisiana State University and
Agricultural and Mechanical College
in partial fulfillment of the
requirements for the degree of
Doctor of Philosophy

in

The Department of Chemistry

By
Britney Lyn Hebert
B.S., Nicholls State University, 2011
August 2016

DEDICATION

My parents, Scott and Stephanie Hebert, have been my guiding force throughout my academic career. They have always pushed me and encouraged me to keep reaching higher and without them I would not have achieved such great things in life. I'm so proud to have such wonderful, loving people as my support. I would also like to thank the rest of my family for being my extra reinforcement.

A large amount of gratitude is saved for Dustin Prestridge who has been my rock throughout my journey. Without your emotional support I would not have maintained my sanity. Lastly, to my loving godchild Dylan who always puts a smile on my face.

ACKNOWLEDGEMENTS

I would like to sincerely thank my research advisor, Dr. David Spivak, who gave me an opportunity in his research group. Because of my time spent in his group, I have learned how to solve problems and tackle new projects.

I would also like to extend my gratitude towards Dr. Doug Gilman and Dr. Donghui Zhang who have been great teachers and advisors. My undergraduate researcher, Sarah Powell, has been a great contributor to my research this past year and her help was greatly appreciated. To my many colleagues throughout the years I extend my thanks, especially Dr. Wei Bai, Dr. Nicholas Gariano, and Dr. Danielle Meador who have been great mentors.

Table of Contents

LIST OF TABLES

LIST OF FIGURES

LIST OF SCHEMES

LIST OF ABBREVIATIONS

MIP	Molecularly imprinted polymer
L-NALA	N-α-bismethacryloyl-L-alanine
NOBE	N, O-bismethacryloyl ethanolamine
MAA	Methacrylic acid
EGDMA	Ethylene glycol dimethacrylate
TRIM	Trimethylolpropane trimethacrylate
α	Separation factor, two analytes from one sample
α’	Separation factor, two analytes from different samples
k’	Capacity factor
t_v	Void volume
t_0	Analyte volume
OMNiMIPs	One monomer molecularly imprinted polymers
Bio-MIPs	Biological molecularly imprinted polymers
BASA	Boronate affinity sandwich assay
SERS	Surface-enhanced Raman scattering
IgG	Immunoglobulin G
SPR	Surface plasmon resonance
MBAA	Methylene bisacrylamide
NIPAM	N-isopropylacrylamide
AM	Acrylamide
SELEX	Systematic evolution of ligands by exponential enrichment
PCR	Polymerase chain reaction
PAA	Poly(acrylic acid)
ATRP	Atom transfer free radical polymerization
ASPV	Apple stem pitting virus
HPLC	High performance liquid chromatography
GC	Gas Chromatography

CE	Capillary electrophoresis
SFC	Super critical fluid chromatography
SN_1	Unimolecular nucleophilic substitution
C_b	Bound template
C_f	Free template
RaceMIP	Racemic imprinted polymers
ScaleMIP	Scalemic imprinted polymers
DCM	Dichloromethane
DMAP	4-Dimethylaminopyridine
DCC	N,N'-Dicyclohexylcarbodiimide
DCU	Dicyclohexylurea
PDMS	Poly(N,N-dimethylaminoethyl methacrylate)
PEG	Polyethylene glycol
Sp18	18-atom hexa-ethyleneglycol spacer
MS	Mass spectrometry
DPV	Differential pulse voltammetry
G/C	Guanine and Cytosine content
T_m	Melting temperature
M	Salt concentration
PDMS	Polydimethylsiloxane
PETA	Pentaerythritol triacrylate
TMPTMP	Trimethylolpropane tris(3-mercaptopropionate)
TEMED	Tetramethylethylenediamine
APS	Ammonium persulfate
NIP	Non-Imprinted polymer
d_0	Original length of the hydrogel
d	Length of the hydrogel in response to analyte
NaCl	Sodium chloride

TA	Thiol-acrylate
GLaDiS	Gel laser diffraction sensor
$MgSO_4$	Magnesium sulfate
HCl	Hydrochloric acid
$NaHCO_3$	Sodium bicarbonate
THF	Tetrahydrofuran
LAH	Lithium aluminum hydride
AIBN	Azobisisobutyronitrile
ACVA	4,4′-Azobis(4-cyanovaleric acid)
NEA	(S)-(−)-1-(1-Naphthyl)ethylamine

ABSTRACT

Molecularly Imprinted Polymers (MIPs) encompass a wide range of applications by changing the different components, e.g. the template, crosslinker or functional monomers. Of interest among these different applications are separations and sensors.

Separations by MIPs traditionally use a chiral pure template but in some cases that chiral pure template may not be available for imprinting. Using chiral (N-α-bismethacyloyl-L-alanine) and achiral (N,O-bisacrylamide ethanolamine) crosslinkers we investigated imprinting of scalemic and racemic template mixtures of Boc-tyrosine enantiomers. The achiral and chiral crosslinkers yielded similar results for the partial separation of enantiomers by scalemic imprinted polymers because separation and recognition are not dependent on diastereomeric interactions here. The racemic imprinted polymers, however, required the chiral crosslinker for chiral differentiation. Surprisingly, variable D or L bias was observed in the L-NALA racemic imprints with equal probability over multiple replicates of polymer synthesis. The binding of the template to the polymer was evaluated in both batch rebinding and chromatographic modes, and the results will be discussed in detail.

Another important area of MIPs is their applicability in sensor devices, especially for biological targets. A proven method of development of a sensor by molecular imprinting is by incorporating MIPs in a stimuli-responsive hydrogel. An imprinted hydrogel was developed to detect a DNA mir21 mimic using complementary aptamers in both a capillary hydrogel format and thin film hydrogel diffraction grating. The hydrogels imprinted for the DNA mir21 target were responsive to the re-introduction of the target sequence and selective among similar nucleotide sequences. It was also shown that a full pre-polymer complex of both the aptamers

with the DNA mir21 mimic was necessary to achieve maximum stimuli response detected by shrinking of the hydrogel sensor.

CHAPTER 1 INTRODUCTION TO MOLECULAR IMPRINTING AND ITS COMPONENTS FOR ENANTIOMER SEPARATIONS AND BIOLOGICAL SENSORS

1.1 Molecularly Imprinted Polymers

Molecular Imprinting Polymers (MIPs) is a method to replicate selective binding seen in biological receptors. The molecular recognition in MIPs arises from the creation of selective binding sites and is similar to the "lock and key" fit of enzymes and substrates. The first example of imprinting was by Polyakov, who investigated the use of silica for chromatography back in 1931.[1] In these studies he discovered the selective absorption of additives like toluene, xylene, and benzene to silica treated with these compounds. When the silica was dried, consequently removing the additives, a rigid matrix was left behind that exhibited selective reabsorption of the solvents. The molecular imprinting methods more commonly used today was developed by Wulff in the 1970's. He set out to design polymers with catalytic sites that were similar in function to an enzyme's active site. In this fashion he wanted to simulate the non-covalent and covalent interactions that lead to the specific recognition and binding of an enzyme to its substrate.[2,3] From there, the world of imprinting began to expand from their use in catalysis to various other areas of research.

Imprinting, as depicted in Figure 1.1, makes use of functional monomers and template(s) (a); those functional monomers will preorganize around the template(s) to form a complex (b); a crosslinker can then be added that is responsible for binding site formation and the solution is then polymerized by either photo or thermal polymerization (c). The template can be subsequently removed, leaving an empty binding cavity that is specific to that same template (d) and capable of binding and removal of the template.

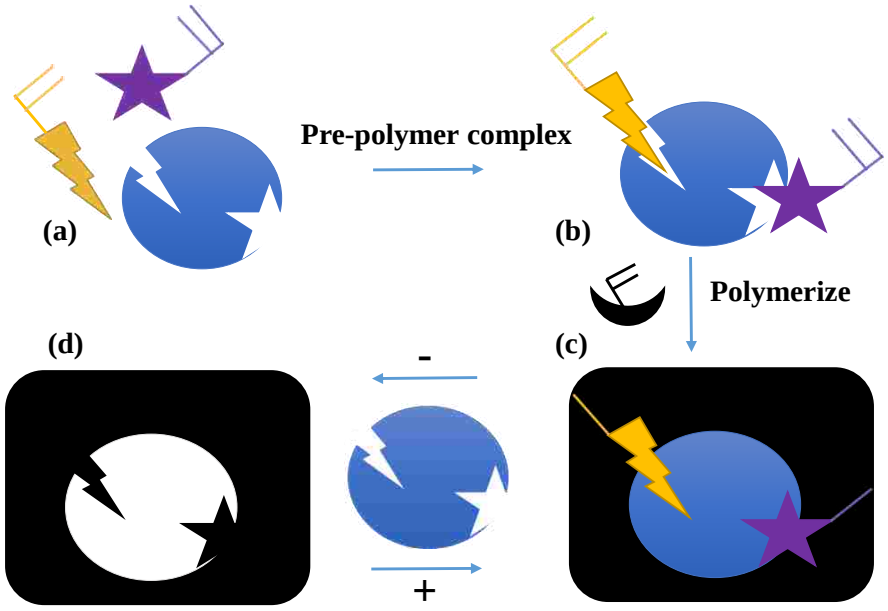

Figure 1.1 Traditional Imprinting scheme

1.1.1 Effects of Changing the Imprinting Components: Functional Monomers

Some of the various areas that imprinting has been instrumental in are separations, sensors, and catalysis. A MIP contains many different components as depicted above which lends itself to several structural changes and advances in applications. Using different templates can lead to various avenues of recognition. For example, MIPs have been applied to selectively bind a range of targets from dendrimers to amino acids.[4-6] In order to establish these different imprinted systems the components need to be adjusted accordingly.

Functional monomers are responsible for the recognition of the template molecules by covalent or noncovalent interactions. MIPs can use a covalent imprinting approach where the template is bound to the polymer network by covalent bonds. By this method, the template and functional monomers are covalently bound and the template can be released by cleaving the bonds, leaving an empty binding site. Upon re-addition of the template to the MIP, the covalent bonds can be re-formed. The covalent approach is useful because it yields high affinity sites and

high binding capacity to the imprinted polymer. However, the biggest disadvantage of this form of imprinting is the limitation of reversible bond forming functional groups i.e. disulfides and ketals. Breaking the covalent bonds also requires chemical treatment which may degrade the polymer providing a harsh environment for any type of biological imprinting.

The majority of imprinting applications however use noncovalent interactions (Figure 1.1) which are more versatile. Noncovalent imprinting relies on interactions such as ion-ion, hydrogen bonding, π-π, dipole-dipole, and Van der Waals forces between the functional monomer and the template. For the noncovalent imprinting there are three different classes of functional monomer: acidic, basic, and neutral. Depending on the template to be imprinted, the functional monomer is chosen using complementary interactions. In the cases of acidic functional monomers, monomers like methacrylic acid (MAA **1**, Figure 1.2) are typically used and are well suited to binding templates with carboxylic acid functionalities.[7-10] Whereas, neutral functional monomers can take advantage of hydrophobic and hydrogen bonding interactions.[11-13] Because of these varying groups many libraries have been established to assist in providing the right functional monomer to template.[14,15] A drawback to these noncovalent imprinting strategies is the production of both high affinity and low affinity binding sites.[16] One approach to eliminate the low affinity binding sites is to use a hybrid imprinting system; imprint using covalent bonding of the template to the functional monomer and after cleaving the template, rebinding relies on noncovalent interactions.[17] However, this pairing may not always be possible or provide improved interactions over the covalent and non-covalent approaches between template and MIP.

1.1.2 Effects of Changing the Imprinting Components: Solvent

Polymerization solvent plays a large role in the imprinting effect by aiding in binding interactions and effectively dissolving all of the imprinting components. Solvent, often referred to as the porogen, can enhance complexation in non-covalent imprinting as in the case of separations where the hydrogen bonding and other weak binding are responsible for template-monomer interactions.[18] Before and during polymerization for organic based MIPs, less polar solvents will increase the formation of complexes between the functional monomer and the template. On the other hand, the strong polar solvents like acetic acid can cause dissociation of the hydrogen bonding causing a poor imprinted polymer to be produced, with little or no selectivity for the template.[19] Using the same aprotic solvents from polymerization usually enhance the rebinding of the template to the MIP after polymerization.[20,21]

By contrast, in biological based MIPs it is critical to use an aqueous based media. Especially in the cases of drug delivery where biologically safe solutions are necessary throughout the polymerization to ensure that even after degradation there will be no toxic solvents. Also, biomacromolecules are only stable in aqueous media because they often have very complex tertiary and quaternary structures.

1.1.3 Effects of Changing the Imprinting Components: Crosslinker

Crosslinking in MIPs is also vital to each system as seen for catalysis and separations that rely on formation of binding sites via highly crosslinked systems. In traditional imprinting systems, the polymer is made up of 80-90% crosslinker due to the strong dependence of binding site formation. Some commonly used crosslinkers are ethylene glycol dimethacrylate (EGDMA **2**, Figure 1.2), divinylbenzene (DVB), and trimethylolpropane trimethacrylate (TRIM).

However, for bio-imprinting in some cases the percentage of crosslinker is much smaller to allow for removal and rebinding of the much larger macromolecules. If too much crosslinker is used then the large templates may become permanently encapsulated within the imprinted cavity, such as proteins and viruses that can be up to thousands of KDa's in size; thus the imprinting strategy has to be revised. Depending on the type of system and the means of recognition, different types of crosslinking can be used.

1.2 Separations in MIPs

Enantiomer separations in MIPs are often utilized as the stationary phase material and the molecular recognition element for high performance liquid chromatography (HPLC). For separations by HPLC a more rigid system is required which means less functional monomer can be used. In traditional imprinting, both functional monomers and a crosslinker are incorporated and only 5-20% of the system consists of functional monomer requiring optimization of the ratio between the two components. Many approaches have been investigated to improve on the crosslinker design to maximize its effect. One unique approach was to add some functional properties to the crosslinker to make a hybrid monomer such as N, O-bismethacryloyl ethanolamine (NOBE **3**, Figure 1.2). NOBE contains a crosslinking methacrylate section similar to EGDMA and a functional hydrogen bonding section methacrylamide. NOBE is soluble in organic solvents which, as previously mentioned, is a very pivotal feature; because using polar aprotic solvents helps promote the non-covalent interactions in the complexing of template and monomer.[18]

When imprinted as the crosslinker with MAA as the functional monomer, NOBE's success was originally reported for its ability to surpass an EGDMA/MAA imprinted polymer when imprinted with dansyl-L-phenylalanine as the template. The selectivity of the MIPs by

HPLC is measured as the separation factor (α') (Equation 2), which is a ratio of the capacity factors of the imprinted template over the non-imprinted (k') found from the retention time of the analyte (t_v) and a non-retained sample (t_0) (Equation 1). The new MIPs analyzed resulted in an α' of 2.3 for NOBE/MAA and the EGDMA/MAA imprint a slightly lower value of 1.7.[22]

$$k' = \frac{t_v - t_0}{t_0} \qquad \text{Equation 1}$$

$$\alpha' = \frac{k'_1}{k'_2} \qquad \text{Equation 2}$$

This traditional approach is still very popular in the literature despite the required customization to each system; however, the Spivak research group discovered a new method. This new imprinting technique utilizes NOBE's design having; one monomer as both the crosslinker and functional monomer, known as One MoNomer Molecularly Imprinted Polymers (OMNiMIPs). Most impressive was the OMNiMIPs' advancement over the traditional EGDMA/MAA imprint when NOBE was used as the only crosslinking monomer without MAA, displaying a 3.6 α' value.[23]

In the interest of developing a crosslinking monomer for even better selectivity, several modifications have been made to NOBE's structure. Some of these alterations were in the form of: the addition of a methyl group to give a chiral center (N-α-bismethacryloyl-L-alanine, L-NALA **4**, Figure 1.2), changing the polymerizable groups from methacrylate to acrylate (2-acrylamidoethyl acrylate, **5**), changing the proximity of the hydrogen donor/acceptor groups (2-methyl-N-(3-methyl-2-oxobut-3-enyl) acrylamide, **6**), and incorporating three crosslinking appendages with an extra selective site (1, 3-dimethacrylamidopropan-2-yl methacrylate, **7**). Of interest among the new designs was the chiral monomer derivative L-NALA. L-NALA is not sterically hindered, like its predecessors, and was shown to be successful in single enantiomer imprinting as apparent by its α' of 3.8 when imprinting L-Boc-Tyrosine.[23] It was thought that L-

NALA could be successful when imprinting mixtures of enantiomers because of its potential to form diastereomeric complexes with chiral analytes.

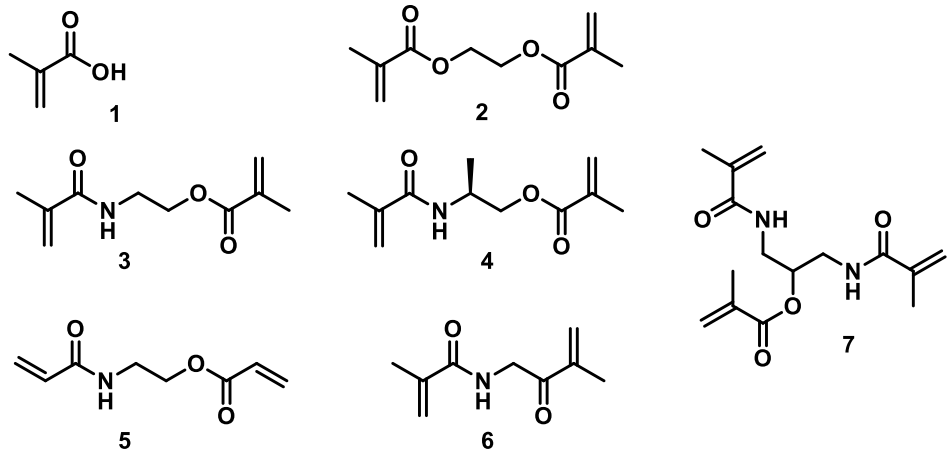

Figure 1.2 Structures of methacrylic acid (1), ethylene glycol dimethacrylate (2), N, O-bismethacryloyl ethanolamine (3), N-α-bismethacryloyl-L-alanine (4), 2-acrylamidoethyl acrylate (5), 2-methyl-N-(3-methyl-2-oxobut-3-enyl) acrylamide (6), and 1, 3-dimethacrylamidopropan-2-yl methacrylate.

Enantiomer separations, of course, require a technique that is capable of differentiating stereoisomers. Some examples of enantiomer separations using HPLC include: polysaccharide-based chiral stationary phases,[24,25] Pirkle-type chiral stationary phases that rely on π-π interactions,[26] hydrogen bonding and dipole-dipole stacking or even chiral ionic liquids that can be used as either stationary phase or mobile phase additives.[27,28] Although these are very useful methods, it can be costly to buy individual columns to tailor each separation or to find the correct mobile phase/analyte interactions.

Typically for chiral separations using MIPs, a single enantiomer is imprinted but for practical use a pure chiral enantiomer may not always be available for imprinting. This is seen many times in pharmaceuticals where a mixture of enantiomers are produced in synthesis reactions. The solution to this would be to imprint the mixture of analytes, for example a racemic (50/50) or scalemic (non-equal) mixture from the pharmaceutical product and separate the

enantiomers using that imprinted mixture as the templates (Figure 1.3). Few examples have been researched for racemic imprinting; however a basis was established by the Hosoya group who utilized Pirkle-type interactions between the functional monomer and the imprinted racemic enantiomer mixture to achieve separation.[29] Scalemic imprinting, however, has not been attempted until recently.[4] Producing a mixture of enantiomers as mentioned is very likely, especially an unknown, unequal mixture of enantiomers. It is vital to establish a protocol that can provide an easy separation to acquire pure enantiomers in this case. A method of imprinting scalemic and racemic mixtures of enantiomers will be discussed in detail in Chapter 2. The imprinting was accomplished using the NOBE and L-NALA crosslinking monomers and Boc-Tyrosine enantiomers as the templates.

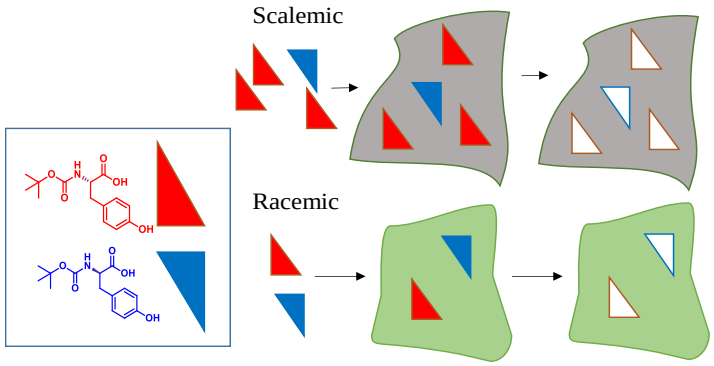

Figure 1.3 Illustration of scalemic and racemic imprinting of enantiomers (L-Boc-tyrosine in red and D-Boc-tyrosine in blue) and the appropriate formed binding sites for each system.

For scalemic imprinting of Boc-tyrosine, both the achiral NOBE and chiral L-NALA were virtually equal in their partial separation of Boc-tyrosine analytes. Thus, chiral separations by scalemic imprinted polymers were determined to rely on an excess number of binding sites for one enantiomer over another and not by diasteomeric interactions. Racemic imprinting on the other hand was only able to yield partial separation by the L-NALA MIPs. This data corresponds with the literature that a chiral selector must be present to differentially recognize enantiomers.

1.3 MIPs for biological imprinting

Among the other avenues of imprinting are biological imprinted polymers (Bio-MIPs). Bio-MIPs require different crosslinking and functional interactions to account for the biological templates. These MIPs have much larger templates; in most cases templates such as viruses or proteins are imprinted and the imprinted networks cannot contain such highly crosslinked systems because of lack of diffusion in and out of the imprinted polymer. This is much different than the formulations previously described for traditional molecular imprinting. Not only does the crosslinking need to be adjusted but also the solution phase. For example, in drug delivery or implanted devices organic solvents may cause cellular damage, therefore it is important to construct a MIP that is hydrophilic. Substituting water for organic solvents, however, weakens non-covalent interactions which has created a hurdle for researchers as the resulting molecular recognition is decreased.[30]

The field of bio-MIPs is rapidly advancing and so are the solutions to creating a sensor material that is compatible and sensitive in aqueous media. For the detection of glycoproteins, Ye et al. created a boronate affinity sandwich assay (BASA) with a formation of layers between the glycoprotein templates, the boronate-affinity MIPs, and boronate-affinity surface-enhanced Raman scattering (SERS) probes.[31] Their system provides an alternative to immunoassays which use antibodies; antibodies are undesirable due to high cost and poor stability. Other examples include: hybrid aptamer MIP nanoparticle sensors using a cocaine analog as a template,[32] ultrathin polymeric films with surface imprints of immunoglobulin G (IgG-MIP) fabricated onto surface acoustic wave (SAW) chips using an electrosynthesis approach,[33] and MIP nanoparticles integrated on a surface plasmon resonance (SPR) sensor chip with microfluidics for capture and

analysis of waterborne viruses.[34] Although these methods are successful sensors for their respective templates, they often require very complex method development.

Another popular method of imprinting biological targets is by incorporating hydrogels which are much simpler and cheaper systems. Hydrogels are crosslinked networks that allow for the absorption of water and are compatible with bio-macromolecules because of their aqueous environment. The crosslinking in hydrogels is also much different than in other MIPs. As mentioned previously, bio-MIPs require less crosslinking resulting in a more porous matrix ideal for diffusion of large targets. It's been demonstrated that the best response of a thrombin imprinted hydrogel was with networks containing less than 1.0 mol% crosslinking relative to the total monomer concentration.[35] The hydrogels thus rely heavily on the functional recognition.

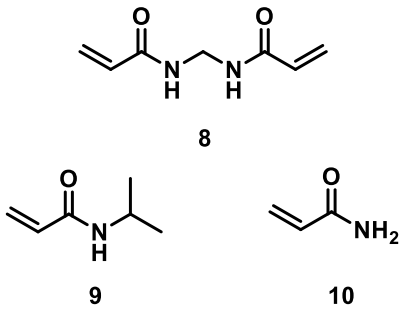

Figure 1.4 Structures of MBAA (8), NIPAM (9), and AM (10).

Although for bio-MIPs the crosslinking is not a major component of the polymer, it is still a much needed support. Depending on the MIP system, the crosslinking could be made by chemical or physical routes. In a radical polymerization, a crosslinker such as methylene bisacrylamide (MBAA **8**, Figure 1.4) can be used. MBAA makes a good candidate for crosslinking in these MIPs due to its solubility in water which is compatible to the desired system and is often incorporated into hydrogels to be imprinted for biological targets. The hydrogel network can be lightly crosslinked with MBAA, creating a more porous network.

Given the decreased amount of crosslinker in these imprints, shape selectivity is lost in the hydrogel; instead the effective imprint is more dependent on preorganization of the functional monomer to the biological template. One portion of the functional composition in hydrogels is comprised of monomers such as N-isopropylacrylamide (NIPAM **9**, Figure 1.4) and acrylamide (AM **10**, Figure 1.4); these monomers are often used in bio-imprinting because they offer a protein-like backbone that provides hydrogen bonding complementarity.[36] An additional piece that is essential to the identification of the biological target from the polymer matrix, is a recognition element similar to the functional monomer in traditional imprinting, e.g. aptamers.

In the case of proteins, viruses, or bacteria, aptamers have been used as an artificial receptor. Aptamers are pieces of oligonucleotides, DNA or RNA, that are capable of binding with high selectivity towards different classes of targets; they are often more stable than their antibody counterparts and cheaper to synthesize. They are developed from a system called S.E.L.E.X or systematic evolution of ligands by exponential enrichment. S.E.L.E.X. is a procedure that involves repetitive rounds of two steps: using an affinity method for partitioning of aptamers from non-aptamers and polymerase chain reaction (PCR) amplification of aptamers.[37,38] Aptamers can easily be modified with a polymerizable group for the incorporation into the hydrogel network for easy target recognition.

Hydrogels are unique systems that can be altered into "smart materials" based on their stimuli responsive behavior. Most appropriate is the ability to shrink or swell in response to a stimulus or molecular recognition of a target. The response of the hydrogels is dependent on the polymers incorporated into the hydrogel allowing the sensor to be tailored to specific templates. A good example of the swelling response was a hydrogel network synthesized with poly(vinyl alcohol)/poly(acrylic acid).[39] Poly(acrylic acid) (PAA) is known for its artificial muscle

behavior in gels because of its super absorbent abilities. These hydrogels exhibited a response of increasing swelling as the pH subsequently increased.

There have been many successful examples of MIP hydrogels. Kuriu et al. employed lectin-imprinted hydrogel layers on surface plasmon resonance sensor chips. The MIP was made by atom transfer radical polymerization (ATRP) grafting from a gold surface to prepare a Concanavalin A imprinted hydrogel.[40] Miyata et al. fabricated a tumor responsive hydrogel that was pre-complexed to polymerizable antibodies that were copolymerized with acrylamide and a crosslinker, poly(ethylene glycol) dimethacrylate.[41] The hydrogels were polymerized in 3mm capillary tubes, removed from the tube and the resulting MIP showed a swelling response upon removal of the glycoprotein target AFP, and exhibited shrinking upon re-addition of the AFP in the 10^{-7} M (micromolar) range.

More impressive are the hydrogel MIPs by Bai et al which had recognition in the 10^{-12} M (femtomolar) range. Similar to the above example by Miyata, the recognition relied on the complexation of aptamers to the protein targets. The complex was polymerized by a redox initiation and remained in capillary tubes where the swelling and shrinking were directly measured using a magnifying glass equipped with a ruler for naked-eye detection. Their system also displayed the importance of both imprinting of the template for recognition and the need for aptamers in selectivity. The technique was applied to two different targets; thrombin, a multifunctional serine protease, and PDGF-ββ, a dimeric protein.[35] The complexation was also successfully applied to imprinting of an impure extract of apple stem pitting virus (ASPV). Here Bai et al. imprinted the ASPV-specific aptamer complex in a patterned mold and the change in response was measured by the given diffraction pattern with a simple laser pointer.[42]

The next avenue of research was to explore the molecular recognition response for short oligonucleotide sequences as targets. There are very few sensors available for short RNA or DNA pieces that are especially cheap and sensitive. Many methods include Mass spectrometry or immunoassays which require large sample quantities and trained technicians to prep and analyze the samples. To find an alternative, the hydrogel MIP system was ideal for an amplified response for a new target, mir21 (a siRNA biomarker). As part of the microRNA family that are naturally occurring noncoding strands, they, on occasion, are overexpressed and are known to become oncogenic.[43] Many researchers have been focusing on ways to suppress these sequences but developing a simple recognition application is still a challenge.

Chapter 3 will discuss the application of the MIP hydrogel developed by the Spivak research group for sensing the DNA mir21 mimic, as the RNA sequence is less stable and more expensive. As for the case of the capillary hydrogels, an optimal formulation of DNA to the crosslinker and functional monomers was found resulting in 5.7 ± 1.8% shrinkage of the gel for a 10^{-8} M (nanomolar) solution of the DNA mir21 target and it was also found to be selective for the target among similar sequences. The DNA mir21 hydrogel was also made by the double-imprinted diffraction-grating method. The method in which to synthesize these grating hydrogels was improved upon resulting in better transfer from the mold material to the hydrogel with reproducibility. After optimization of the grating hydrogels, a maximum shrinkage of 4.4 ± 0.40% was observed. In both methods it was proven that the full A1-DNA mir21-A2 was necessary for optimal response to the DNA mir21 target; signifying both the importance of imprinting and the resulting pre-polymer complexation.

1.4 References

(1) Polyakov, M. V. Adsorption properties and structure of silica gel. *Zhurnal fizicheskoi khimii* **1931**, *2*, 799-804.

(2) Wulff, G.; Sarhan, A. Use of polymers with enzyme-analogous structures for the resolution of racemates. *Angew. Chem., Int. Ed. Engl.* **1972**, *11*, 341.

(3) Wulff, G.; Sarhan, A.; Zabrocki, K. Enzyme-analog built polymers and their use for the resolution of racemates. *Tetrahedron Lett.* **1973**, 4329-4332.

(4) Hebert, B.; Meador, D. S.; Spivak, D. A. Scalemic and racemic imprinting with a chiral crosslinker. *Anal. Chim. Acta* **2015**, *890*, 157-164.

(5) Le Jeune, J.; Spivak, D. A. Analyte separation by OMNiMIPs imprinted with multiple templates. *Biosens. Bioelectron.* **2009**, *25*, 604-608.

(6) Zimmerman, S. C.; Zharov, I.; Wendland, M. S.; Rakow, N. A.; Suslick, K. S. Molecular Imprinting Inside Dendrimers. *J. Am. Chem. Soc.* **2003**, *125*, 13504-13518.

(7) Andersson, L.; Sellergren, B.; Mosbach, K. Imprinting of amino acid derivatives in macroporous polymers. *Tetrahedron Lett.* **1984**, *25*, 5211-5214.

(8) Sellergren, B.; Ekberg, B.; Mosbach, K. Molecular imprinting of amino acid derivatives in macroporous polymers. Demonstration of substrate- and enantio-selectivity by chromatographic resolution of racemic mixtures of amino acid derivatives. *J. Chromatogr.* **1985**, *347*, 1-10.

(9) Dong, H.; Tong, A.-j.; Li, L.-d. Syntheses of steroid-based molecularly imprinted polymers and their molecular recognition study with spectrometric detection. *Spectrochim. Acta, Part A* **2003**, *59A*, 279-284.

(10) Kempe, M. Oxytocin receptor mimetics prepared by molecular imprinting. *Lett. Pept. Sci.* **2000**, *7*, 27-33.

(11) Yu, C.; Mosbach, K. Insights into the origins of binding and the recognition properties of molecularly imprinted polymers prepared using an amide as the hydrogen-bonding functional group. *J. Mol. Recognit.* **1998**, *11*, 69-74.

(12) Zhang, T.; Liu, F.; Chen, W.; Wang, J.; Li, K. Influence of intramolecular hydrogen bond of templates on molecular recognition of molecularly imprinted polymers. *Anal. Chim. Acta* **2001**, *450*, 53-61.

(13) Sreenivasan, K. Effect of the type of monomers of molecularly imprinted polymers on the interaction with steroids. *J. Appl. Polym. Sci.* **1998**, *68*, 1863-1866.

(14) Karim, K.; Breton, F.; Rouillon, R.; Piletska, E. V.; Guerreiro, A.; Chianella, I.; Piletsky, S. A. How to find effective functional monomers for effective molecularly imprinted polymers? *Adv. Drug Delivery Rev.* **2005**, *57*, 1795-1808.

(15) Karlsson, B. C. G.; O'Mahony, J.; Karlsson, J. G.; Bengtsson, H.; Eriksson, L. A.; Nicholls, I. A. Structure and Dynamics of Monomer-Template Complexation: An Explanation for Molecularly Imprinted Polymer Recognition Site Heterogeneity. *J. Am. Chem. Soc.* **2009**, *131*, 13297-13304.

(16) Maier, N. M.; Lindner, W. Chiral recognition applications of molecularly imprinted polymers: a critical review. *Anal. Bioanal. Chem.* **2007**, *389*, 377-397.

(17) Whitcombe, M. J.; Rodriguez, M. E.; Villar, P.; Vulfson, E. N. A New Method for the Introduction of Recognition Site Functionality into Polymers Prepared by Molecular Imprinting: Synthesis and Characterization of Polymeric Receptors for Cholesterol. *J. Am. Chem. Soc.* **1995**, *117*, 7105-7111.

(18) Spivak, D. A. Optimization, evaluation, and characterization of molecularly imprinted polymers. *Adv. Drug Delivery Rev.* **2005**, *57*, 1779-1794.

(19) Sellergren, B.; Shea, K. J. Influence of polymer morphology on the ability of imprinted network polymers to resolve enantiomers. *J. Chromatogr.* **1993**, *635*, 31-49.

(20) Kempe, M.; Mosbach, K. Binding studies on substrate- and enantio-selective molecularly imprinted polymers. *Anal. Lett.* **1991**, *24*, 1137-1145.

(21) Spivak, D.; Gilmore, M. A.; Shea, K. J. Evaluation of Binding and Origins of Specificity of 9-Ethyladenine Imprinted Polymers. *J. Am. Chem. Soc.* **1997**, *119*, 4388-4393.

(22) Sibrian-Vazquez, M.; Spivak, D. A. Enhanced Enantioselectivity of Molecularly Imprinted Polymers Formulated with Novel Cross-Linking Monomers. *Macromolecules* **2003**, *36*, 5105-5113.

(23) Sibrian-Vazquez, M.; Spivak, D. A. Molecular Imprinting Made Easy. *J. Am. Chem. Soc.* **2004**, *126*, 7827-7833.

(24) Okamoto, Y.; Kawashima, M.; Hatada, K. Chromatographic resolution. XI. Controlled chiral recognition of cellulose triphenylcarbamate derivatives supported on silica gel. *J. Chromatogr.* **1986**, *363*, 173-186.

(25) Okamoto, Y.; Aburatani, R.; Fukumoto, T.; Hatada, K. Chromatographic resolution. XVII. Useful chiral stationary phases for HPLC. Amylose tris(3,5-dimethylphenylcarbamate) and tris(3,5-dichlorophenylcarbamate) supported on silica gel. *Chem. Lett.* **1987**, 1857-1860.

(26) Welch, C. J. Evolution of chiral stationary phase design in the Pirkle laboratories. *J. Chromatogr. A* **1994**, *666*, 3-26.

(27) Zhou, Z.; Li, X.; Chen, X.; Hao, X. Synthesis of ionic liquids functionalized β-cyclodextrin-bonded chiral stationary phases and their applications in high-performance liquid chromatography. *Anal. Chim. Acta* **2010**, *678*, 208-214.

(28) Liu, Q.; Wu, K.; Tang, F.; Yao, L.; Yang, F.; Nie, Z.; Yao, S. Amino acid ionic liquids as chiral ligands in ligand-exchange chiral separations. *Chem. - Eur. J.* **2009**, *15*, 9889-9896, S9889/9881-S9889/9889.

(29) Hosoya, K.; Shirasu, Y.; Kimata, K.; Tanaka, N. Molecularly Imprinted Chiral Stationary Phases: Requirement for the Chiral Template. *Anal. Chem.* **1998**, *70*, 943-945.

(30) Nicholls, I. A.; Ramstroem, O.; Mosbach, K. Insights into the role of the hydrogen bond and hydrophobic effect on recognition in molecularly imprinted polymer synthetic peptide receptor mimics. *J. Chromatogr. A* **1995**, *691*, 349-353.

(31) Ye, J.; Chen, Y.; Liu, Z. A Boronate Affinity Sandwich Assay: An Appealing Alternative to Immunoassays for the Determination of Glycoproteins. *Angew. Chem., Int. Ed.* **2014**, *53*, 10386-10389.

(32) Poma, A.; Brahmbhatt, H.; Pendergraff, H. M.; Watts, J. K.; Turner, N. W. Generation of Novel Hybrid Aptamer-Molecularly Imprinted Polymeric Nanoparticles. *Adv. Mater. (Weinheim, Ger.)* **2015**, *27*, 750-758.

(33) Tretjakov, A.; Syritski, V.; Reut, J.; Boroznjak, R.; Opik, A. Molecularly imprinted polymer film interfaced with Surface Acoustic Wave technology as a sensing platform for label-free protein detection. *Anal. Chim. Acta* **2016**, *902*, 182-188.

(34) Altintas, Z.; Gittens, M.; Guerreiro, A.; Thompson, K.-A.; Walker, J.; Piletsky, S.; Tothill, I. E. Detection of Waterborne Viruses Using High Affinity Molecularly Imprinted Polymers. *Anal. Chem. (Washington, DC, U. S.)* **2015**, *87*, 6801-6807.

(35) Bai, W.; Gariano, N. A.; Spivak, D. A. Macromolecular Amplification of Binding Response in Superaptamer Hydrogels. *J. Am. Chem. Soc.* **2013**, *135*, 6977-6984.

(36) Sellergren, B.; Hall, A. J. In *Tilte*2012; John Wiley & Sons Ltd.

(37) Drolet, D. W.; Jenison, R. D.; Smith, D. E.; Pratt, D.; Hicke, B. J. A high throughput platform for systematic evolution of ligands by exponential enrichment (SELEX). *Comb. Chem. High Throughput Screening* **1999**, *2*, 271-278.

(38) Musheev, M. U.; Krylov, S. N. Selection of aptamers by systematic evolution of ligands by exponential enrichment: Addressing the polymerase chain reaction issue. *Anal. Chim. Acta* **2006**, *564*, 91-96.

(39) Jin, X.; Hsieh, Y.-L. pH-responsive swelling behavior of poly(vinyl alcohol)/poly(acrylic acid) bi-component fibrous hydrogel membranes. *Polymer* **2005**, *46*, 5149-5160.

(40) Kuriu, Y.; Kawamura, A.; Uragami, T.; Miyata, T. Formation of thin molecularly imprinted hydrogel layers with lectin recognition sites on SPR sensor chips by atom transfer radical polymerization. *Chem. Lett.* **2014**, *43*, 825-827.

(41) Miyata, T.; Hayashi, T.; Kuriu, Y.; Uragami, T. Responsive behavior of tumor-marker-imprinted hydrogels using macromolecular cross-linkers. *J. Mol. Recognit.* **2012**, *25*, 336-343.

(42) Bai, W.; Spivak, D. A. A Double-Imprinted Diffraction-Grating Sensor Based on a Virus-Responsive Super-Aptamer Hydrogel Derived from an Impure Extract. *Angew. Chem., Int. Ed.* **2014**, *53*, 2095-2098.

(43) Kilic, T.; Erdem, A.; Erac, Y.; Seydibeyoglu, M. O.; Okur, S.; Ozsoz, M. Electrochemical Detection of a Cancer Biomarker mir-21 in Cell Lysates Using Graphene Modified Sensors. *Electroanalysis* **2015**, *27*, 317-326.

CHAPTER 2 ACHIRAL VERSUS CHIRAL CROSSLINKING MONOMERS USED FOR MOLECULARLY IMPRINTED CHIRAL ENANTIOMERS

2.1 Introduction of Achiral and Chiral Crosslinking monomers

The field of molecular imprinting has vastly expanded since its discovery over 40 years ago.[1] Molecular Imprinting came about as a synthetic mimic to nature's ability to selectively bind an antigen to an antibody. The first account of imprinting, and what is still used today, incorporates a crosslinker, functional monomers, a template molecule and an initiator. This is referred to as traditional imprinting and typically uses a non-interactive crosslinker such as ethylene glycol dimethacrylate (EGDMA, 2) to create a non-bonding scaffold which supports a binding site and uses functional monomers such as methacrylic acid (MAA, 1) (Figure 2.1). The traditional approach requires optimization of many variables such as the EGDMA, MAA and template ratios along with the choice of mobile phase. A less complicated system was discovered which is referred to as One MoNomer Molecularly Imprinted Polymers (OMNiMIPs), merging the crosslinking and functionality into one monomer for the same or better selectivity for its imprinted template. Here, the ratios of crosslinker to monomer do not have to be adjusted because the system only requires one monomer. The first OMNiMIP made used the crosslinker N, O-bismethacryloyl ethanolamine or NOBE (Figure 2.1, 3); it can form hydrogen bonding interactions and crosslink due to its methacrylamide and methacrylate groups, respectively.

NOBE is an achiral crosslinker, which can limit its imprinting ability. For example, while NOBE has proven to successfully imprint chiral pure enantiomers and distinguish between them, it cannot be employed for chiral discrimination when imprinting a racemic template.[2-4] However, there is a great need to imprint racemic or scalemic (a mixture that is not one to one) ratios of enantiomer templates.

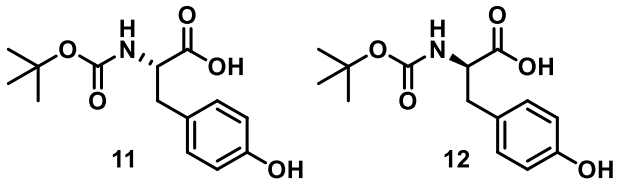

Figure 2.1 Structures of **11** L-Boc-tyrosine and **12** D-Boc-tyrosine

Chiral pure compounds (e.g. natural products) are few in comparison to the vast amount synthesized in pharmaceuticals that require specific chirality.[5-8] For pharmaceuticals it is of special importance to have the pure enantiomer; because approximately half of these synthesized compounds are chiral molecules.[9,10] Stereochemistry in drugs can make a difference in effectiveness or side effects because each enantiomer may react at different rates in the presence of enzymes that have different affinities for chiral substrates. [10] For example, in the investigation of antidepressant drugs it was found that the racemate of a drug can be used while in other cases it was discovered that a single enantiomer is needed such as the case for citalopram. Citalopram was commercially available as the racemic mixture of (+)-S and (-)-R enantiomers; however it was found that the R enantiomer inhibited the activity of the S enantiomer making the drug ineffective. As a result the drug is now administered as the chiral pure S enantiomer known as escitalopram.[11] Another example is in the form of an anti-nausea drug known as thalidomide. Thalidomide has very different acting enantiomers; the R-enantiomer promotes sleep and relieves anxiety while the S-enantiomer has been linked to over 2,000 still births in women who took it while pregnant.[10]

There is a vast collection of organic reactions that have been developed that have stereochemical outcomes that can be understood and sometimes controlled to synthesize chiral products. A few well-known examples are the nucleophilic substitution (SN_1) and Diels Alder reaction which both give racemic products.[12] A problem that arises from reactions producing

mixtures of enantiomers is the required separation of those chiral products. Enantiomer separation can be achieved by various chiral modifications of many analytical methods. Among these separation methods are liquid chromatography (LC), gas chromatography (GC), capillary electrophoresis (CE) and super critical fluid chromatography (SFC) to name a few.[13] While these techniques work well they are limited by the chiral selectors available and the selector-ligand combinations to be established. Finding the appropriate pairing of the selector for one of the enantiomers of a chiral mixture requires extensive empirical experimentation, and a selector system found may still not be 100% effective.[14]

An alternative method of chiral separations uses MIPs designed as stationary phases for HPLC. As opposed to the other chiral separation methods mentioned, MIPs are straightforward to synthesize, inexpensive and require less optimization, especially if OMNiMIPs are used. MIPs are widely used for HPLC, but as previously mentioned have been limited by the availability of a single enantiomer to imprint.[2-4,15] This limits use of MIPs for newly synthesized products that may not have a pure isolated enantiomer to imprint. For that reason, it is of importance to synthesize a MIP that can imprint using a (i.e. racemic or scalemic) mixture of template. For HPLC the selective ability of the MIP is determined by a normalization factor denoted as the capacity factor (k') (Equation 1). The capacity factor is a function of the retention times where the t_v is the retention volume of the analyte and t_0 is the dead volume usually determined by acetone since it should not bind to the stationary phase. The k' can be calculated for any non-imprinted analytes as well as the imprinted analyte. These k' values can further be used in the calculation of the selective ability of the MIP; analyzed as the separation factors (α or α') (Equation 2). The separation factor is the ratio of k' values, the most retained analyte (k'_1) over the least retained (k'_2). The separation factor can be used in two separate cases; when analytes

are injected on the HPLC simultaneously as racemic or scalemic mixtures it is denoted as α and when the analytes are injected separately on the HPLC it is referred to as α'. When evaluating the separation factors, a larger α or α' indicates a greater separation by the MIP.

$$k' = \frac{t_v - t_0}{t_0} \qquad \text{Equation 1}$$

$$\alpha' = \frac{k'_1}{k'_2} \qquad \text{Equation 2}$$

Batch rebinding is another method commonly used for MIPs to study the affinity distributions and thermodynamic parameters of analyte binding to the polymer material (Figure 2.2). Batch rebinding differs in respect to HPLC in that it allows the polymer material to reach equilibrium with the analytes. Whereas with HPLC there can be non-equilibrium conditions, for example analytes may not have the ability to adequately bind to all of the available sites at the mobile phase flow rates that are used. The batch rebinding technique provides information on affinity constants and distributions of the analyte by isotherms that can be represented in logarithmic form with respect to the analyte bound (C_b) to the polymer versus the analyte still free in solution (C_f). The isotherms yield information about the binding of the polymer through parameters such as the slope and magnitude of binding affinity. For example, isotherms between imprinted versus the non-imprinted (or strongly imprinted versus weakly imprinted) polymers have different isotherm sloping.[16-19]

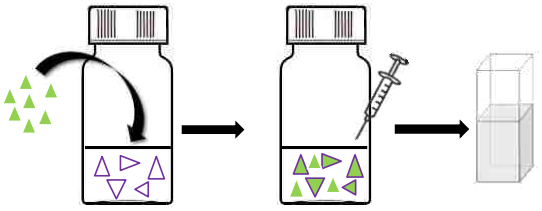

Figure 2.2 Batch rebinding process: starting with various concentrations of the template (green) are added to a vial containing the polymeric material (purple). The template and polymer are allowed to reach equilibrium and the free template in solution can then be extracted out and measured by UV/Vis.

There have only been three examples of racemic imprinted polymers to date and up to this point there were no examples of scalemic imprinting before the studies described here. Among the examples of racemic imprinting was an OMNiMIP developed by the Spivak research group using L-NALA and Boc-tyrosine enantiomers. This was the first introduction of L-NALA as a crosslinking monomer, but in this case it did not show any selectivity for the enantiomers imprinted.[20] The other two cases of racemic imprinting were more successful but were limited. Torres et. al. used a non-crosslinking chiral carboxylate monomer but was restricted to imprinting amine based targets, such as the bis(1-phenylethyl)amine enantiomers that was used.[21] The final example was by the Hosoya group who synthesized a non-crosslinking functional monomer that could form Pirkle-type diastereomeric interactions with nitro-aromatic derivatized chiral amines.[22] Pirkle columns can be useful for enantiomer separations but they are specific to separating only certain analytes because they rely on π-π stacking in fortuitous cases. These last two examples are also a traditional imprinting approach using EGDMA as their non-interactive crosslinker whereas the OMNiMIP system was used for Chapter 2's approach.

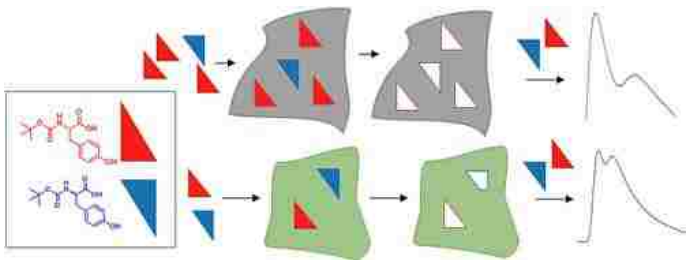

Figure 2.3 Imprinting of scalemic (top) and racemic (bottom) using Boc-tyrosine enantiomers and the resulting chromatograms for racemic analytes. Reprinted with permission

The topics covered in this chapter investigate the capability of both the achiral NOBE and the chiral L-NALA monomer to imprint racemic (RaceMIP) and scalemic (ScaleMIP) mixtures

of Boc-tyrosine. Separation was shown to occur, or at least partial separation of these enantiomers (Figure 2.3), in the chromatographic mode. The structure of Boc-tyrosine is seen in Figure 2.1 entry 5 and 6 and is regularly used in imprinted studies because of its intermediate size. With respect to biological importance, L-tyrosine acts as a positive regulator of melanogenesis (production of melanin) in some species and regulates other cellular functions as well.[23] Low amounts of D-tyrosine are found in the body, however high concentrations can result in interference of biosynthesis or biological action of vital neurotransmitters such as dopamine among other conditions.[24] Therefore, it is of biological importance to develop sensor materials that can detect tyrosine enantiomers or similar compounds, especially in the case where they are administered together.

2.2 Racemic Imprinting Results for Crosslinking Monomers

An in-depth look at the racemic imprinting of the achiral NOBE versus the chiral L-NALA monomers for making OMNiMIPs was studied. Both NOBE and L-NALA were imprinted with a racemic (50/50) mixture of L-and D-Boc-tyrosine and the performance for enantioseparation is presented below in Table 2.1. It was hypothesized that the NOBE-RaceMIP would be ineffective due to its achiral nature and inability to produce chiral discrimination via diastereomeric interactions; and this was true as seen by the effective separation factor (α') of 1.0, indicating there was no separation or selectivity of enantiomers (entry 1 in Table 2.1). For racemic imprinting all properties of NOBE complexes with Boc-tyrosine analytes are equal for each enantiomer including: formation of equal numbers of pre-polymer complexes, the number of binding sites formed as a function of the pre-polymer complex concentration, and rebinding affinity of the template to the polymer for each enantiomer. This results in the predictable lack of enantioseletivity of the NOBE-RaceMIP.

Table 2.1 HPLC data for NOBE and L-NALA RaceMIPs*

Polymer Identifier	Entry	Template	k'_L	k'_D	α'
NOBE-RaceMIP	1	Racemic Boc-Tyr	4.7	4.5	1.0
L-NALA-RaceMIP1**	2	Racemic Boc-Tyr	2.9	4.5	1.6 (D)
L-NALA-RaceMIP2	3	Racemic Boc-Tyr	3.7	5.1	1.4 (D)
L-NALA-RaceMIP3	4	Racemic Boc-Tyr	4.2	3.1	1.4 (L)
L-NALA-RaceMIP4	5	Racemic Boc-Tyr	4.5	4.0	1.1 (L)
L-NALA-RaceMIP5	6	Racemic Boc-Tyr	8.1	7.1	1.14 (L)

*HPLC conditions: particle size 25–37 μm; column 100 x 2.1; mobile phase, MeCN/acetic acid (99:1); analytes (1mM Boc-L-tyrosine, 1 mM Boc-D-tyrosine, acetone (used to determine void volume)) were all detected at 260 nm; flow rate 0.1 mL/min; sample volume injected 5 μL.

The L-NALA monomer provided the opportunity for enantioseparation of racemic mixtures because of the diastereomeric interactions possible with other enantiomeric template compounds. In the same manner as the NOBE-RaceMIP, L-NALA was imprinted with a racemic mixture of Boc-tyrosine (L-NALA-RaceMIPs, entries 2-6 in Table 2.1) and to accurately investigate the results of imprinting a racemic mixture, five replicate polymers with the same formulation were synthesized. For the L-NALA-RaceMIPs enantioselectivity was observed; however, it was revealed that there was a bias in the retention for either the L or D enantiomers in seemingly equal proportions as seen by the capacity factors (k') in Table 2.1.

Table 2.2 Analyte concentration and flow rate data for L-NALA-RaceMIP2 and L-NALA-RaceMIP3.*

Polymer Identifier	Entry	Boc-Tyr concentration	Flow Rate mL/min	k'_L	k'_D	α'
L-NALA-RaceMIP2	1	5 mM	0.1	4.2	4.2	1.0
	2	2 mM	0.1	3.7	4.6	1.2
	3	1 mM	0.1	3.7	5.1	1.4

L-NALA-RaceMIP3	4	1 mM	0.5	3.9	4.0	1.0
	5	1 mM	1.0	2.4	2.6	1.1
	6	5 mM	0.1	3.3	3.4	1.0
	7	2 mM	0.1	4.0	3.2	1.3
	8	1 mM	0.1	4.2	3.1	1.4
	9	1 mM	0.5	3.6	3.6	1.0
	10	1 mM	1.0	2.9	2.8	1.0

*HPLC conditions: particle size 25–37 μm; column 100 x 2.1; mobile phase, MeCN/acetic acid (99:1); analytes (1mM Boc-L-tyrosine, 1 mM Boc-D-tyrosine, acetone (used to determine void volume)) were all detected at 260 nm; flow rate 0.1 mL/min; sample volume injected 5 μL.

At this time there is no explanation for the switching biased behavior of the L-NALA-RaceMIPs, but upon further investigations it was revealed that once the polymer displayed a bias it did not change even when the analyte concentration or flow rate (Table 2.2) was changed. In the case of flow rate for L-NALA-RaceMIP2 and L-NALA-RaceMIP3 (entries 3-5 and 8-10, respectively) as the flow rate was decreased, the α' increased but the bias for the same enantiomer remained the same; however, at higher flow rate there was a loss of selectivity. This is a known effect of MIPs that has been ascribed to increased residence time of substrates diffusing through the polymer affording greater exposure of the substrate to binding sites within the bulk of the polymer.[25] The same observation can also be seen by concentration studies (entries 1-3 and 6-8) where the imprinted polymers keep the enantioselective bias of the analytes; and as the concentration of analytes was decreased the α' improved.

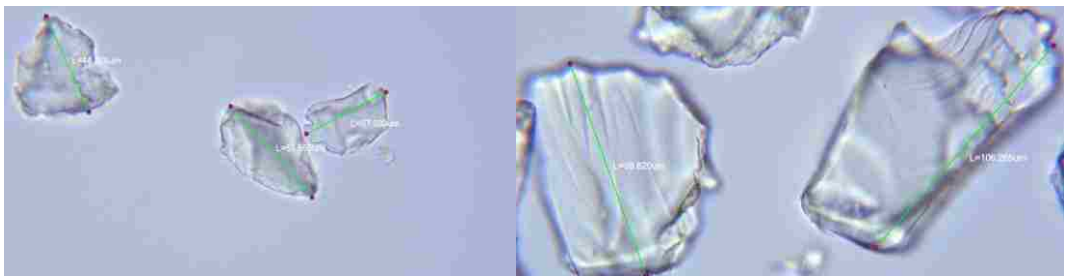

Figure 2.4 Microscope Images of L-NALA-RaceMIP3 (a) 25-38 (b) 38-45μm.

The results for each material by HPLC analyses can be seen in Table 2.3. The smallest size, entry 1, column was packed differently because of available material, with a smaller column length of 50 mm in comparison to 100 mm that was used for the larger sized particles, and at a higher concentration of analyte of 2 mM instead of the 1 mM a larger α' was obtained (contrary to the trend observed in Table 2.2 for 25-38 μm material). Notably the bias switched giving a higher k', longer retention, for the 2mM L-Boc-Tyr (entry 1 (a)) with reference to the 25-38μm material (entry 2) but the α' value for this material (entry 1 a) was quite insignificant indicating no improvement in selectivity. Given the low separation value this could be a negligible occurrence and should be replicated with an additional L-NALA-RaceMIP imprint. However, the bias switching in this was shown to be unlikely by entry 1 (b) with an α' of 1.04 when analyzing 1 mM samples, where the original enantiomeric favorability was observed for the D-Boc-tyr analyte. In typical HPLC separations smaller sized material is desired because you have more stationary phase that can more uniformly pack into the column and more surface area for analytes to come in contact resulting in more theoretical plates and higher efficiencies (inverse relationship between theoretical plates and stationary phase size). For MIPs on the other hand, they rely on diffusion of analytes through the polymer material and into the binding sites. For smaller MIP stationary phase material, like entry 1, loss in selectivity could due to the destruction of a significant number of high-affinity sites or density changes in the polymer that limit access of substrates to the binding sites.[25]

Table 2.3 Effect of polymer size and column length on enantioselectivity.*

Size	Entry	Concentration	k'_L	k'_D	α'
20-25 μm**	1 a	2 mM	4.0	4.3	1.1
	1 b	1 mM	4.7	5.0	1.0
25-38 μm	2	1 mM	8.1	7.1	1.1
38-45 μm	3	1 mM	5.3	5.1	1.0

25-38 μm[+]	4	2mM	8.7	7.4	1.2

[*]HPLC conditions: column 100 x 2.1; mobile phase, MeCN/acetic acid (99:1); analytes (1mM Boc-L-tyrosine, 1 mM Boc-D-tyrosine, acetone (used to determine void volume)) were all detected at 260 nm; flow rate 0.1 mL/min; sample volume injected 5 μL. [**]column 50 x 2.1 mm. [+]column size 250 x 2.1 mm and flow rate 0.2 mL/min.

There was no enhancement of the separation factor by the larger size (entry 3) but the D-Boc-tyr bias remained the same. These results could be attributed to inaccessible binding sites for the analytes by the larger material, by not accessing more high affinity binding sites when grinding the material. The sizing does not seem to change the bias of the D- or L-Boc-tyrosine analytes indicating no correlation between the switching of enantiomeric favorability and the size of the material; which implies that bias is not formed during the grinding process.

One last condition that was studied was the effect of column size. L-NALA-RaceMIP5 sized 25-38μm was packed into a 250 x 2.1 mm column, entry 4 of Table 2.3. This was also not a direct comparison because the concentration of analytes used was 2 mM and also the flow rate was faster at 0.2 mL/min to compensate for the column size. The larger sized column did give a higher α' of 1.2, this was expected since there are more theoretical plates which improves resolution; however, it does not have an effect on the biasing enantiomer. The L-Boc-tyrosine bias remained the same in this case indicating that the change in volume of the polymeric materials used for analysis does not change the affinity bias for one enantiomer over the other.

After closely studying the effects on HPLC which is under kinetic conditions of flow rate, it was of importance to look at the thermodynamics of the polymer-enantiomer interactions using batch rebinding. Batch rebinding studies were used to establish whether a consistent bias could be seen under equilibrium conditions providing thermodynamic values that are more reliable than conditions affected by kinetics. In other words, batch rebinding allows the imprinted material to reach equilibrium with the analyte before binding measurements are taken;

where-as HPLC is under constant flow during measurements and mass transfer of the analyte between the stationary phase and solution phase may not be complete. The batch rebinding results can be interpreted using isotherms of the analytes in the form of log-log plots (Figure 2.4). L-NALA-RaceMIPs previously studied (in Table 2.2) were used again in the batch rebinding studies for direct comparison to the HPLC results.

The graphs for both L-NALA-RaceMIPs (Figure 2.5 (a) and (b)) give linear outputs in the log-log plots of the binding isotherms. This was anticipated based on log-log plots reported for various other molecularly imprinted polymers in the literature.[17,26-30] However, it is important to note that for both L-NALA-RaceMIPs the relative slopes of the isotherm lines representing the L and D enantiomers on each of the polymers are different. In Figure 2.5 (a), there are two fitted lines, one corresponding to the isotherm of L-Boc-Tyr and the other for D-Boc-Tyr, that do not have the same slope indicating different binding behavior for each enantiomer on the same RaceMIP. This type of behavior has also been seen in the literature for most of the MIPs reported using the log-log plotting isotherms.[19,26-28,31-35] The difference in slopes is a known result for imprinted polymers arising from different binding affinity distributions for each enantiomer.[17-19] The reason for inconsistent preference for L or D enantiomers described above could be due to the fact that the difference in slopes causes the L and D isotherms to intersect, as shown in Figures 2.5 a and b. It can be expected that at the intersection, the preference for binding one enantiomer over the other will change as a function of concentration.

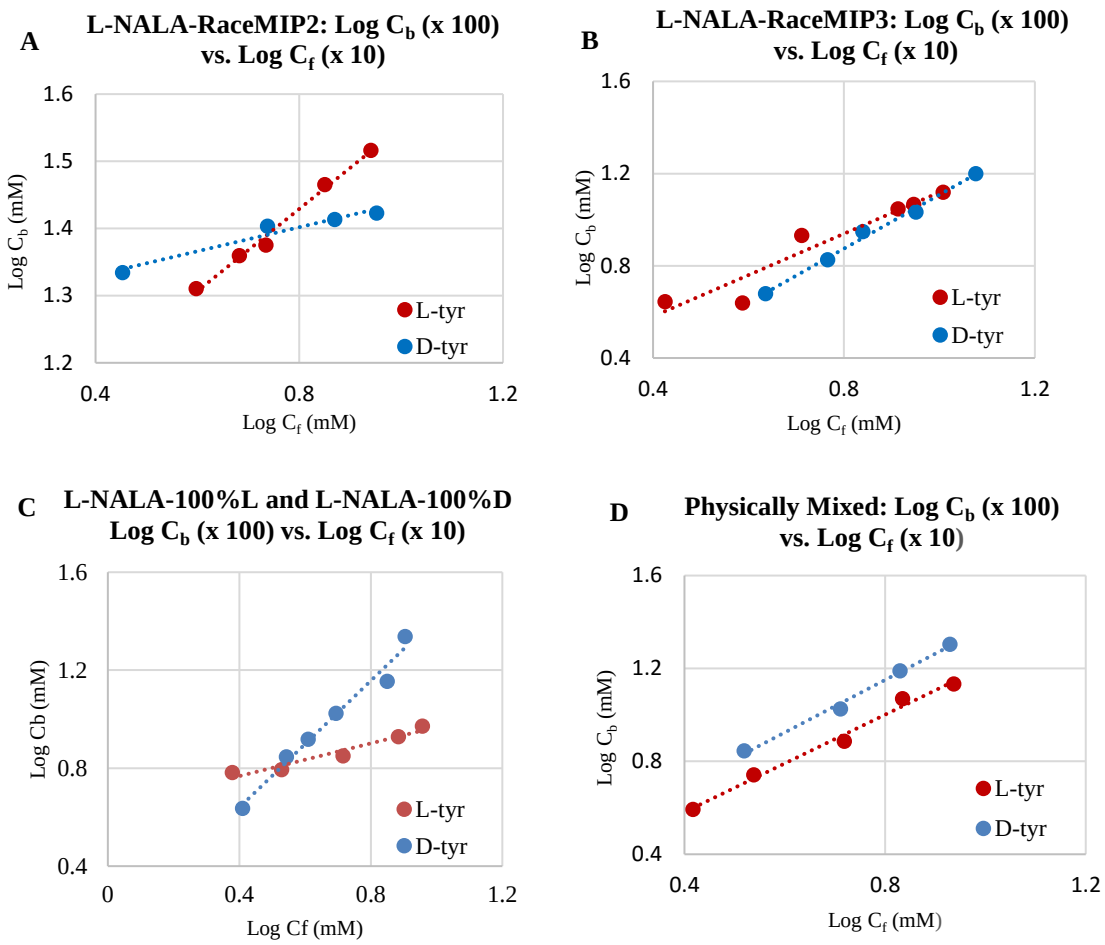

Figure 2.5 Log-log plots of isotherms fit to the Freundlich isotherm, comparing batch rebinding of tBoc-Tyr enantiomers on (A) L-NALA-RaceMIP2, (B) L-NALA-RaceMIP3, (C) L-NALA-100%L and D, and the (D) physically mixed material comprised of 50/50 (w/w) L-Boc-Tyr and D-Boc-Tyr imprinted polymers.

As shown in Table 2.2 however, that is not the case for HPLC because there is overloading of the column or the system is not under equilibrium and those concentration effects cannot be observed. Entry c was an experiment carried out as a prerequisite to (D) of Figure 2.5, to see the behavior of separately imprinted pure enantiomers. The MIPs from Table 2.4 entries 1 and 2 were evaluated separately by batch for their selectively of their imprinted enantiomer, for example the L-NALA imprinted with pure L-Boc-tyr (entry 1, MIP-100% L) was studied with L-Boc-tyr, and vice versa (entry 2). From this study it was seen that the L-NALA imprints each

enantiomer differently, even when imprinted independently, indicating the existence of different reactivity or interactions between the monomer and each of the enantiomers.

As a last comparison to the L-NALA-RaceMIP binding affinities, a control stationary phase (Table 2.4 entry 3) was created by physically mixing equal amounts (50/50 : w/w) of pure L-Boc-Tyr (Table 2.4 entry 1) imprinted polymer with pure D-Boc-Tyr (Table 2.4 entry 2) imprinted polymer. This physically mixed stationary phase was intended to mimic the racemic imprinting process.

Table 2.4 Comparison of α' for L-NALA imprinted with single enantiomers, single enantiomer imprints mixed together, and a Racemic NALA mixture imprinted with a single enantiomer.

Polymer Identifier	Entry	Template	k'_L	k'_D	α'
MIP-100% L	1	L-Boc-Tyr	6.2	2.0	3.1
MIP-100% D	2	D-Boc-Tyr	2.3	7.3	3.0
Physically Mixed	3	50/50 (w/w) L- & D-Boc-Tyr MIPs	3.6	4.7	1.3
[D-NALA + L-NALA] (50/50 : w/w)	4	L-Boc-Tyr	5.1	2.4	2.1

*HPLC conditions: particle size 25–37 μm; column 100 x 2.1; mobile phase, MeCN/acetic acid (99:1); analytes (1mM Boc-L-tyrosine, 1 mM Boc-D-tyrosine, acetone (used to determine void volume)) were all detected at 260 nm; flow rate 0.1 mL/min; sample volume injected 5 μL.

Both polymers should provide equal numbers of L- and D-Boc-Tyr imprinted sites, and should in theory give the same results as the L-NALA-RaceMIP. However, that this was not the case and batch rebinding isotherms of the physically mixed stationary phase showed parallel slopes (Figure 2.5 (d)), which indicates identical binding affinity distributions for each enantiomer. The greater uptake for the "D" imprinted material versus the "L" imprinted polymer is explained by direct match to the larger capacity factor for the "D" imprinted polymer (k'_D = 7.3 in Table 2.4, entry 2) versus the "L" imprinted polymer (k'_L =6.2, entry 1). For the chromatographic results of the column packed with the mixed stationary phase, the larger

capacity factor of the "D" imprinted material also gives rise to the greater retention for D-Boc-Tyr versus L-Boc-Tyr. Thus, the physically mixed stationary phase acts in a predictable manner, combining directly the properties of the two different imprinted polymers for both batch rebinding and chromatographic results.

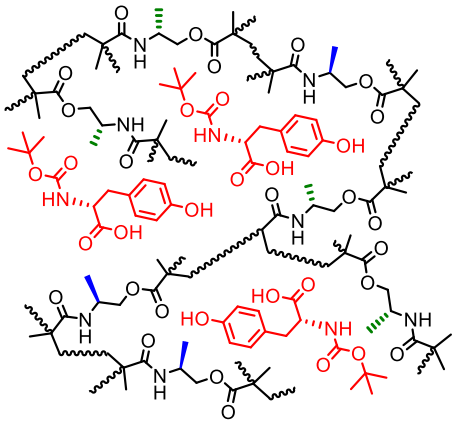

Figure 2.6 Imprinted network of racemic NALA crosslinker with L-Boc-tyr template.

For comparison to the L-NALA-RaceMIPs, a polymer was synthesized using a racemic crosslinking monomer comprised of D-NALA and L-NALA with pure L-Boc-Tyr as the template (Table 2.4 entry 4 and Figure 2.6). The resulting racemic crosslinking material gave an α' value of 2.1. While this α' value is higher than the L-NALA imprinted with racemic Boc-Tyr, it's still lower than the α' value of 3.0 for pure L-Boc-Tyr imprinted using L-NALA. These results show that imprinting using a racemic mixture of template or racemic crosslinker curbs the chiral recognition of the imprinted polymers; however, racemic templates appear to have a much more severe effect on lowering the enantioselectivity of imprinted materials.

Lastly, experiments were conducted to determine whether the L-NALA-RaceMIPs performed better when used as OMNiMIPs (Table 2.1 entries 2-6) or copolymerized with ethyleneglycol dimethacrylate (EGDMA, **1**) which provides an inert scaffold for holding the L-NALA-template interactions in place and allowing L-NALA to act as the functional monomer.

As shown in Figure 2.7, when racemic Boc-Tyr was imprinted using a crosslinker ratio of 25 mol% L-NALA and 75 mol% EGDMA, an α' of 1.05 was obtained, indicating a lack of enantiomer separation. However, as the amount of L-NALA was increased, the α' value increased until the highest average α' value of 1.4 was obtained for the 100% L-NALA MIP. These results confirm that for imprinting racemic enantiomers, selectivity is improved when imprinting as an OMNiMIP.

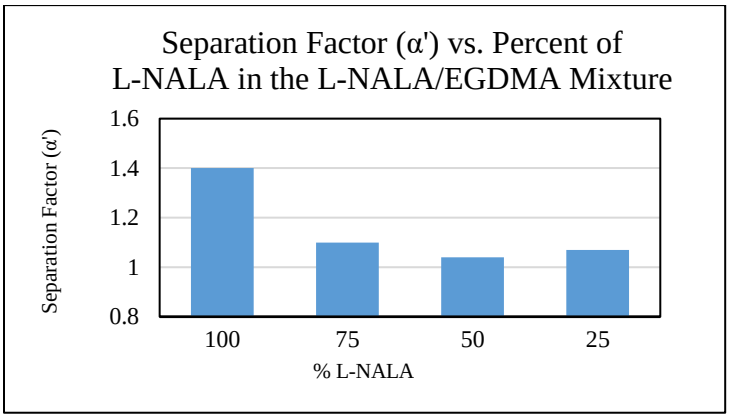

Figure 2.7 OMNiMIP performance using L-NALA for racemic Boc-Tyr imprinting versus MIPs made using a more traditional formulation incorporating a mixture of monomers (L-NALA and EGDMA).

2.3 Scalemic Imprinting with an Achiral Crosslinker

Scalemic imprinting of chiral enantiomers (Scheme 2.1) has not been reported in the literature prior to the work presented here that was recently published.[36] The MIPs presented herein were made using NOBE as the crosslinking monomer and scalemic mixtures of Boc-Tyr as the templates, identified as NOBE-ScaleMIPs. The purpose was to evaluate if the chiral crosslinker (L-NALA) is also necessary for scalemic imprinting or if the same selectivity could be achieved using the simpler achiral monomer (NOBE).

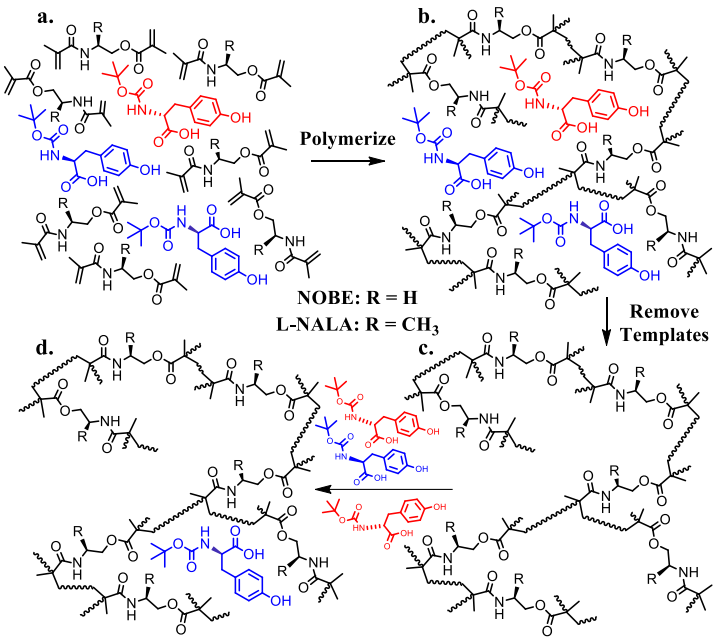

Scheme 2.1 Representation of molecular imprinting a scalemic template mixture using L-NALA or NOBE crosslinkers and the resulting selectivity.

The results for the NOBE-ScaleMIPs (entries 1-2) can be seen in Table 2.5 along with the reprint of L-NALA-ScaleMIPs' (entries 3-4) data for direct comparison.36 Both NOBE-ScaleMIPs gave effective separation factors in the 1.5-1.8 range; and a significant observation was that binding is selective for the enantiomer that is in excess in the template mixture; i.e. the L-Boc-Tyr is more strongly bound to the 50% ee NOBE-ScaleMIP-L (entry 1), and vice versa (entry 2).

The enantioselectivity seen is presumably due to production of an increased number of binding sites for the L enantiomer that proportionally results in longer retention of the L enantiomer over D. This verifies the utility of NOBE OMNiMIPs for scalemic imprinting. The chromatogram cascades for the NOBE-ScaleMIPs can be seen in Figures 2.6 and 2.7 where it shows partial separation for scalemic and racemic mixtures that matches what has been seen for L-NALA.

Table 2.5 NOBE and L-NALA[36] scalemic imprinted polymers with Boc-tyrosine as the template mixture.*

Polymer Identifier	Entry	Template	k'_L	k'_D	α'
NOBE-ScaleMIP-L	1	75 % L; 25 % D	5.4	3.5	1.5
NOBE-ScaleMIP-D	2	25 % L; 75 % D	3.1	5.6	1.8
L-NALA-ScaleMIP-L**	3	75 % L; 25 % D	3.8	2.5	1.5
L-NALA-ScaleMIP-D**	4	25 % L; 75 % D	2.1	3.6	1.7

*HPLC conditions: particle size 25–37 μm; column 100 x 2.1; mobile phase, MeCN/acetic acid (99:1); analytes (1mM Boc-L-tyrosine, 1 mM Boc-D-tyrosine, acetone (used to determine void volume)) were all detected at 260 nm; flow rate 0.1 mL/min; sample volume injected 5 μL.

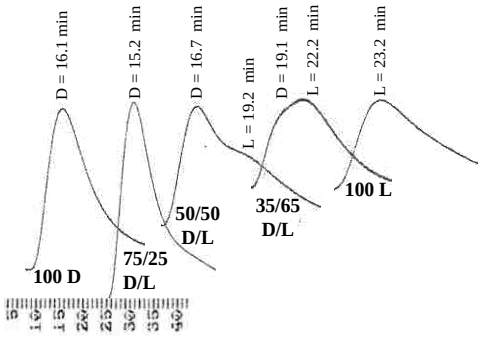

Figure 2.8 NOBE-ScaleMIP-L chromatographic cascades of Boc-Tyr analytes.

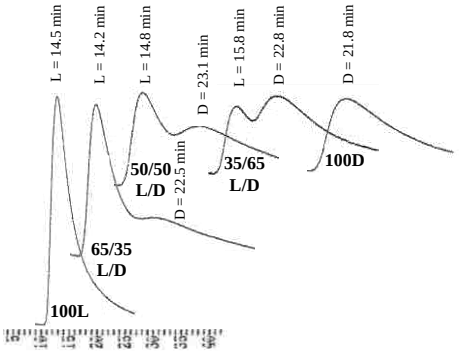

Figure 2.9 NOBE-ScaleMIP-D chromatographic cascades of Boc-Tyr analytes.

Scalemic imprinting using the chiral crosslinker L-NALA was initially thought to have an advantage because of its ability to form diastereomeric pre-polymer complexes with the L and D enantiomers of Boc-Tyr. Potentially, this could have an advantage toward biasing affinity of the binding sites preferentially for the L or D enantiomer of the template.

However, entries 3 and 4 in Table 2.5 for the L-NALA-ScaleMIPs give α' values similar to the corresponding entries in Table 2.5 for L- and D-ScaleMIPs synthesized using the achiral NOBE crosslinker. This result discounts any significant influence of crosslinker chirality on the overall scalemic imprinting process. In addition, there is only a small influence on the

enantioselectivity by the crosslinker chirality, seen by the comparable values of L-NALA OMNiMIPs made with 100% L- or D-Boc tyrosine as template (Table 2.4). This was also supported by the NMR studies where no diastereomeric bias was seen for the solution phase complexes of L-NALA with L-and D-Boc-Tyr.[36]

2.4 Racemic and Scalemic Enantiomer Imprinting Conclusions

A comprehensive comparison of scalemic and racemic imprinted polymers was evaluated using OMNiMIPs fabricated from a chiral (L-NALA) and non-chiral (NOBE) crosslinker. To the best of our knowledge this is the first report of scalemic imprinted polymers, and an initial focus was to determine whether a chiral crosslinker would enhance selectivity by materials that were imprinted with a scalemic mixture of enantiomers. The results were nearly identical for the chiral L-NALA-based polymers and the achiral NOBE-based polymers for imprinting a scalemic (50% ee) mixture of Boc-Tyr, which showed partial resolution of scalemic and racemic mixtures in chromatographic mode. Based on these findings, the selectivity in these materials was reasoned to be a result of an increased number of binding sites for the major isomer, and not by diastereomeric interactions that could exist between the chiral crosslinker and the template enantiomers. Support for this conclusion came from 1H NMR studies that showed equivalent shifts of the N-H peak for L-NALA in the presence of D- and L-Boc-Tyr.[36]

For imprinting a racemic mixture (i.e. RaceMIPs), a difference in chiral selectivity was observed when the chiral L-NALA crosslinker was used, versus polymers imprinted with the achiral NOBE crosslinker which did not show any chiral selectivity at all. When L-NALA was used in combination with EGDMA as a co-crosslinker, the enantioselectivity decreased, showing L-NALA imprinting works best as an OMNiMIP. Partial chromatographic separation was achieved by the L-NALA-RaceMIPs; however, roughly half of the imprinted polymers gave

better retention for D-Boc-Tyr, while the other half consistently bound L-Boc-Tyr better. The underlying mechanism for the chromatographic bias for one enantiomer or the other for each RaceMIP is not clear, however a basic understanding of the behavior of these RaceMIPs has been linked to the binding affinity distribution properties of these materials determined by batch rebinding isotherms. This was seen by the different binding affinity distributions for each enantiomer owing to the strongly or weakly formed imprinted sites formed.

Optimization of HPLC parameters revealed that slower flow rate and lower concentrations improved α' values. Thus it has been shown that the L-NALA-RaceMIPs have equal performance to previously reported racemic imprinted polymers;[21,22] however, baseline chromatographic resolution of enantiomers remains a goal for the future development of chiral crosslinkers. Because both the RaceMIPs and the ScaleMIPs can be developed within a day, this provides a facile route toward determination of the % ee of the racemate or scalemate used for imprinting, using peak deconvolution for any overlapping peaks.

2.5 Future Work

The next step in this project is the development of a new crosslinker incorporating two steoreocenters (Figure 2.8) This is anticipated to be beneficial for racemic imprinting toward achieving better resolution of enantiomers by increasing the number of chiral interactions between the monomer and template.

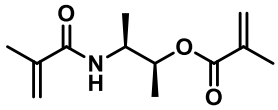

Figure 2.10 New crosslinker,

2.6 Experimental Work

Synthesis of Crosslinking Monomers

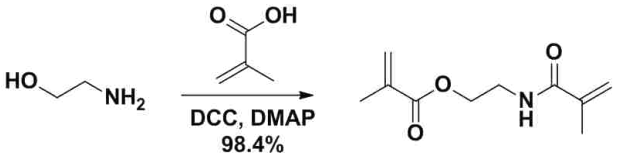

Scheme 2.2 Synthesis of NOBE, details outlined below

N, O-bismethacryloyl ethanolamine

The synthesis of NOBE was similar to a published protocol.[4,20] Ethanolamine (1 eq.) and dichloromethane (DCM) were added to a 500 mL roundbottom and allowed to cool to 0°C. This was followed by the addition of 4-dimethylaminopyridine (DMAP, 0.2 eq.), methacrylic acid (MAA, 2.2 eq.), and dicyclohexylcarbodiimide (DCC, 2.1 eq.). Slowly, the mixture warmed to room temperature and remained stirring for two days. The white dicyclohexylurea (DCU) was filtered off by vacuum filtration leaving the organic solution that was then washed with 1 N HCL (aq) (3 x 100 mL) and saturated $NaHCO_3$ (aq) (6 x 100 mL). Magnesium sulfate ($MgSO_4$) was used to dry the organic layer and yielded an oil after the solvent was evaporated (98 % yield). 1H NMR ($CDCl_3$, 400 MHz) δ ppm 6.41 (1H, br, NH), 6.06 (1H, s), 5.64 (1H, s), 5.54 (1H, s), 5.27-5.25 (1H, d, J= 8 Hz), 4.25-4.22 (2H, t, J= 6 Hz), 3.58-3.54 (2H, q), 1.90 (3H, s), 1.88 (3H, s.) 13C NMR (CDCl3, 100MHz) δ ppm 168.46, 167.65, 139.78, 135.94, 126.20, 119.76, 63.36, 39.22, 18.58, 18.29.

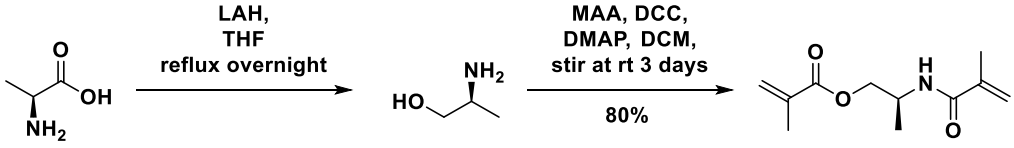

Scheme 2.3 Synthesis of L-NALA, details outlined below

N-α-bismethacryloyl-L-alanine

The crosslinker L-NALA was synthesized by collecting dry tetrahydrofuran (THF) in 500 mL roundbottom and cooling it to 0°C followed by adding lithium aluminum hydride (LAH, 1

eq.). After the temperature was allowed to equilibrate, L-alanine (1 eq.) was slowly added to the roundbottom and was refluxed overnight. The reaction was quenched with saturated potassium carbonate (aq) (20 mL) and the THF was removed via vacuum filtration yielding a colorless oil (70% yield). 1H NMR ($CDCl_3$, 400 MHz) δ ppm 3.55 (m, 1H), 3.23 (m, 1H), 3.01 (m, 1H), 2.01 (br, 3H), 1.06 (s, 3H). 13C NMR (CDCl3, 100MHz) δ ppm 6827, 48.22, 20.09.

The resulting alcohol, L-alaninol (1 eq.) was added into a 500 mL roundbottom with DCM and cooled to 0°C. After, MAA (2.5 eq.) and DMAP (0.2 eq.) were added and after five minutes DCC (2 eq.) was also added to the mixture. The reaction was slowly warmed to room temperature and continued to stir for two days. The DCU was vacuum filtered off followed by washing with 0.5 N HCl (aq) (3 x 50 mL) and saturated $NaHCO_3$ (aq) (4 x 50 mL). The remaining organic layer was dried over $MgSO_4$ and purified by column chromatography with 50/50 EtOAc/hexane (80% yield). 1H NMR ($CDCl_3$, 400 MHz) δ ppm 6.12 (s, 1H), 6.01 (br, 1H), 5.99 (s, 1H), 5.66 (s, 1H), 5.59 (s, 1H) 4, 4.39-4.36 (m, 1H), 4.16-4.09 (m, 2H), 1.94 (s, 6H), 1.24 (d, 3H, 4Hz). 13C NMR ($CDCl_3$, 100MHz) δ ppm 171.14, 167.89, 140.02, 135.93, 126.16, 119.51, 67.10, 44.89, 18.56, 18.27, 17.31.

Polymerization of Crosslinking monomers

The monomer (1.0 g) was added to a 13 x 100 mm glass tube along with solutions of Boc-Tyr (5 mol% with respect to monomer) in 1.3 mL acetonitrile. The initiator AIBN (1.0 mol% with respect to monomer) was added into the solution and purged with nitrogen for five minutes. To seal the system, the glass tube was capped, wrapped with Teflon tape, and overlayed with Parafilm. The glass tube was inserted into a photoreactor apparatus and submerged in a water bath where the temperature was maintained at 21°C. The tube with the solution mixture was then exposed to a 450 W mercury arc lamp surrounded by a borosilicate jacket for 8 hours

immersed in the water bath along with the polymer mixture. To remove the polymer, the glass test tube was broken with a hammer and the particle monolith removed. The resulting polymer was lightly crushed into pieces in the 1-5mm size range and placed in a Soxhlet extraction apparatus charged with methanol for two days to remove the template(s). Using U.S.A. Standard Testing Sieves the polymer was further sized to 25-38 μm after grinding with mortar and pestle and slurried with acetone. The sized polymer was slurry-packed into a stainless steel column (100 mm x 2.1mm i.d.) for analysis by HPLC (Hitachi L-7000 series equipped with L-7100 pump, L-7400 detector and L-7500 integrator) in a 99/1 acetonitrile/acetic acid mobile phase.

Batch rebinding studies

For batch rebinding the dry sized (25-38 μm) polymer material (50 mg) was placed into scintillation vials. In each scintillation vial filled with polymer, various concentrations (0.4 mM-1.6 mM) of L- or D-Boc-Tyr solutions (2 mL) in 99/1 acetonitrile/acetic acid were added. The mixture was lightly shaken by hand every 2-3 hours for the first 8 hours, and allowed to sit overnight (16 hours) in order to reach equilibrium. An aliquot of the solution was removed and the absorbance directly measured by UV spectroscopy (Cary 50 UV-Vis spectrophotometer) at 278 nm. The imprinted polymer material was regenerated by washing with acetonitrile until a peak at 278 nm no longer remained in the supernatant.

2.7 References

(1) Wulff, G. Fourty years of molecular imprinting in synthetic polymers: origin, features and perspectives. *Microchim. Acta* **2013**, *180*, 1359-1370.

(2) Le Jeune, J.; Spivak, D. A. Analyte separation by OMNiMIPs imprinted with multiple templates. *Biosens. Bioelectron.* **2009**, *25*, 604-608.

(3) Meng, A. C.; Le Jeune, J.; Spivak, D. A. Multi-analyte imprinting capability of OMNiMIPs versus traditional molecularly imprinted polymers. *J. Mol. Recognit.* **2009**, *22*, 121-128.

(4) Sibrian-Vazquez, M.; Spivak, D. A. Molecular Imprinting Made Easy. *J. Am. Chem. Soc.* **2004**, *126*, 7827-7833.

(5) Boeckman, R. K.; Editor: *Comprehensive Chirality, Volume 3: Synthetic Methods II-Chiral Auxiliaries*; Elsevier B.V., 2012.

(6) Cossy, J. R.; Editor: *Comprehensive Chirality, Volume 1: Biological Significance-Pharmacology, Pharmaceutical, Agrochemical*; Elsevier B.V., 2012.

(7) Mulzer, J.; Editor: *Comprehensive Chirality, Volume 2: Synthetic Methods I-Chiral Pool and Diastereoselective Methods*; Elsevier B.V., 2012.

(8) Tranter, G. E.; Editor: *Comprehensive Chirality, Volume 8: Separations and Analysis*; Elsevier B.V., 2012.

(9) Sekhon, B. S. Enantioseparation of chiral drugs - an overview. *Int. J. PharmTech Res.* **2010**, *2*, 1584-1594.

(10) Sekhon, B. S. Exploiting the power of stereochemistry in drugs: an overview of racemic and enantiopure drugs. *J. Mod. Med. Chem.* **2013**, *1*, 10-36.

(11) Nageswara Rao, R.; Guru Prasad, K. Stereo-specific LC and LC-MS bioassays of antidepressants and psychotics. *Biomed. Chromatogr.* **2015**, *29*, 21-40.

(12) Daniels, R.; Grady, L. T.; Bauer, L. Mechanisms of cleavage of heteroaromatic ethers. III. The acid-catalyzed cleavage of (S)-(+)-2-(1'-methylheptoxy)pyrimidine. *J. Org. Chem.* **1966**, *31*, 1790-1792.

(13) Scriba, G. K. E.; Editor: *Chiral Separations: Methods and Protocols, Second Edition. [In: Methods Mol. Biol. (N. Y., NY, U. S.), 2013; 970]*; Springer, 2013.

(14) Maier, N. M.; Franco, P.; Lindner, W. Separation of enantiomers: needs, challenges, perspectives. *J. Chromatogr. A* **2001**, *906*, 3-33.

(15) Suedee, R.; Songkram, C.; Petmoreekul, A.; Sangkunakup, S.; Sankasa, S.; Kongyarit, N. Direct enantioseparation of adrenergic drugs via thin-layer chromatography using molecularly imprinted polymers. *J. Pharm. Biomed. Anal.* **1999**, *19*, 519-527.

(16) Wulff, G.; Grobe-Einsler, R.; Vesper, W.; Sarhan, A. Enzyme-analog built polymers, 5. The specificity distribution of chiral cavities prepared in synthetic polymers. *Makromol. Chem.* **1977**, *178*, 2817-2825.

(17) Rushton, G. T.; Karns, C. L.; Shimizu, K. D. A critical examination of the use of the Freundlich isotherm in characterizing molecularly imprinted polymers (MIPs). *Anal. Chim. Acta* **2005**, *528*, 107-113.

(18) Sajonz, P.; Kele, M.; Zhong, G.; Sellergren, B.; Guiochon, G. Study of the thermodynamics and mass transfer kinetics of two enantiomers on a polymeric imprinted stationary phase. *J. Chromatogr. A* **1998**, *810*, 1-17.

(19) Rampey, A. M.; Umpleby, R. J., II; Rushton, G. T.; Iseman, J. C.; Shah, R. N.; Shimizu, K. D. Characterization of the Imprint Effect and the Influence of Imprinting Conditions on Affinity, Capacity, and Heterogeneity in Molecularly Imprinted Polymers Using the Freundlich Isotherm-Affinity Distribution Analysis. *Anal. Chem.* **2004**, *76*, 1123-1133.

(20) LeJeune, J.; Spivak, D. A. Chiral effects of alkyl-substituted derivatives of N,O-bismethacryloyl ethanolamine on the performance of one monomer molecularly imprinted polymers (OMNiMIPs). *Anal. Bioanal. Chem.* **2007**, *389*, 433-440.

(21) Torres, J. J.; Gsponer, N.; Ramirez, C. L.; Vera, D. M. A.; Montejano, H. A.; Chesta, C. A. Experimental and theoretical studies on the enantioselectivity of molecularly imprinted polymers prepared with a chiral functional monomer. *J. Chromatogr. A* **2012**, *1266*, 24-33.

(22) Hosoya, K.; Shirasu, Y.; Kimata, K.; Tanaka, N. Molecularly Imprinted Chiral Stationary Phases: Requirement for the Chiral Template. *Anal. Chem.* **1998**, *70*, 943-945.

(23) Slominski, A.; Zmijewski, M. A.; Pawelek, J. L-tyrosine and L-dihydroxyphenylalanine as hormone-like regulators of melanocyte functions. *Pigm. Cell Melanoma Res.* **2012**, *25*, 14-27.

(24) Friedman, M. Chemistry, Nutrition, and Microbiology of D-Amino Acids. *J. Agric. Food Chem.* **1999**, *47*, 3457-3479.

(25) Simon, R.; Houck, S.; Spivak, D. A. Comparison of particle size and flow rate optimization for chromatography using one-monomer molecularly imprinted polymers versus traditional non-covalent molecularly imprinted polymers. *Anal. Chim. Acta* **2005**, *542*, 104-110.

(26) Sajonz, P.; Kele, M.; Zhong, G.; Sellergren, B.; Guiochon, G. Study of the thermodynamics and mass transfer kinetics of two enantiomers on a polymeric imprinted stationary phase. *Journal of Chromatography A* **1998**, *810*, 1-17.

(27) Umpleby, R. J.; Baxter, S. C.; Rampey, A. M.; Rushton, G. T.; Chen, Y.; Shimizu, K. D. Characterization of the heterogeneous binding site affinity distributions in molecularly imprinted polymers. *J. Chromatogr. B: Anal. Technol. Biomed. Life Sci.* **2004**, *804*, 141-149.

(28) Wu, X.; Goswami, K.; Shimizu, K. D. Comparison of monofunctional and multifunctional monomers in phosphate binding molecularly imprinted polymers. *J. Mol. Recognit.* **2008**, *21*, 410-418.

(29) Tamayo, F. G.; Casillas, J. L.; Martin-Esteban, A. Evaluation of new selective molecularly imprinted polymers prepared by precipitation polymerization for the extraction of phenylurea herbicides. *Journal of Chromatography A* **2005**, *1069*, 173-181.

(30) Turiel, E.; Perez-Conde, C.; Martin-Esteban, A. Assessment of the cross-reactivity and binding sites characterisation of a propazine-imprinted polymer using the Langmuir-Freundlich isotherm. *Analyst (Cambridge, United Kingdom)* **2003**, *128*, 137-141.

(31) Rushton, G. T.; Karns, C. L.; Shimizu, K. D. A critical examination of the use of the Freundlich isotherm in characterizing molecularly imprinted polymers (MIPs). *Anal. Chim. Acta* **2005**, *528*, 107-113.

(32) Torres, J. J.; Gsponer, N.; Ramirez, C. L.; Vera, D. M. A.; Montejano, H. A.; Chesta, C. A. Experimental and theoretical studies on the enantioselectivity of molecularly imprinted polymers prepared with a chiral functional monomer. *Journal of Chromatography A* **2012**, *1266*, 24-33.

(33) Ng, S. M.; Narayanaswamy, R. Molecularly imprinted polymers as optical sensing receptors: Correlation between analytical signals and binding isotherms. *Anal. Chim. Acta* **2011**, *703*, 226-233.

(34) Torres, J. J.; Montejano, H. A.; Chesta, C. A. Characterization of Imprinted Microbeads Synthesized via Minisuspension Polymerization. *Macromol. Mater. Eng.* **2012**, *297*, 342-352.

(35) Baggiani, C.; Giraudi, G.; Giovannoli, C.; Tozzi, C.; Anfossi, L. Adsorption isotherms of a molecular imprinted polymer prepared in the presence of a polymerizable template. Indirect evidence of the formation of template clusters in the binding site. *Anal. Chim. Acta* **2004**, *504*, 43-52.

(36) Hebert, B.; Meador, D. S.; Spivak, D. A. Scalemic and racemic imprinting with a chiral crosslinker. *Anal. Chim. Acta* **2015**, *890*, 157-164.

CHAPTER 3 BIOLOGICAL IMPRINTED HYDROGELS FOR DNA DETECTION

3.1 Introduction Biological Imprinted Hydrogels

Recognition, quantification, and sensing of biological compounds are an important and fast growing field of research. The abundance of biological species is the driving force behind the large area of research conducted to understand how each component may affect the human body and the surrounding environment. These species consist of viruses, proteins, DNA, RNA, and bacteria among many others and there are a wide variety of devices used to detect and quantify these species. A biological sensor can be defined as a device that responds to a physical or chemical stimulus by producing a signal in return. In some cases it may be life-saving to detect a certain species easily and with very little cost to the manufacturer and user.

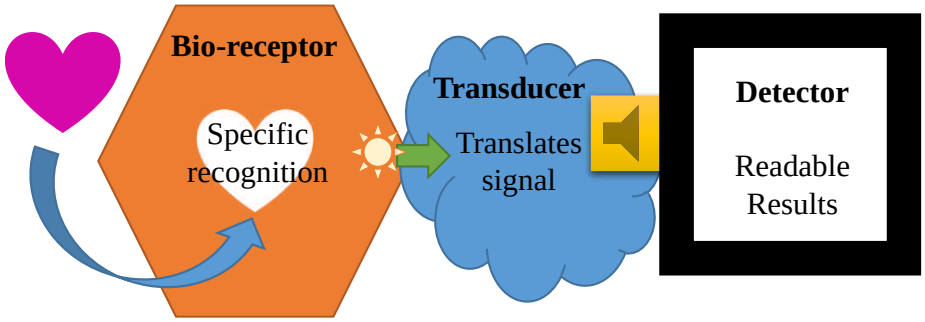

Figure 3.1 Bio-sensor components

The basic components of a biological sensor are depicted in Figure 3.1. In most instances there are three elements: the bio-receptor that is capable of specifically recognizing a target of interest, a transducer that translates the recognition into a signal and a detector that can give readable results. The bio-receptor contains a component for recognition, in some cases by incorporating a substrate that is specific to a particular enzyme of interest; such as β-galactosidase for lactose and chymosin for K-casein.[1,2] A synthetic replacement for recognition

of the bio-receptor is the use of aptamers. Aptamers are DNA or RNA strands that bind to selective molecules (e.g. proteins, viruses, and toxins) with high binding affinity to a specific section or structure of a target made possible by a technique called S.E.L.E.X. (systematic evolution of ligands by exponential enrichment).[3,4]

A biological sensor should be able to specifically recognize the target at abnormal biological concentrations within a high background matrix (having additional samples other than the analyte). It should also be capable of withstanding repeated washing and repetitions without being easily degraded. Biological sensors are typically very costly, for example methods such as mass spectrometry (MS) and immunoassays used for sensing mycotoxins or surface plasmon resonance sensors (SPR) for pathogens, proteins, toxins, and etc.[5,6] Using an instrument like MS is not only expensive, but also requires trained personnel to run; ideally, it is also desired for the practitioner to have a portable and easy to operate bio-sensor.

Hydrogels constitute a desirable bio-sensor in that it incorporates all the features of a typical bio-sensor in one system i.e. recognition, signal translation and readable detection. Hydrogels are loosely defined as crosslinked networks that are capable of retaining water. A hydrogel is neither a liquid nor a solid and can be either chemically or physically crosslinked depending on the application.[7,8] Hydrogels have been used since the 1960s when discovered by Wichterle and Limand.[9,10] These networks have proven to be very versatile for systems such as drug delivery vehicles to autocatalytic enzyme reactions capable of controlling gelation.[11-13]

Hydrogels are an excellent scaffold for a polymeric detection device because they have the ability to change properties based on stimuli such as pH, chemical, mechanical, heat, light or temperature depending on the hydrogel's structural components (i.e. monomers, polymerization conditions, and crosslink density).[14-16] The properties changed can be an alteration of the

hydrophilic/hydrophobic balance, a release of a small molecule or a conformation change such as a swelling or shrinking response of the gel.[17] An example of a stimuli responsive hydrogel would be one incorporated with poly(*N*,*N*-dimethylaminoethyl methacrylate) (PDMA) or poly(ethylene glycol) (PEG) that can give pH responsive behavior. Similarly adding a monomer such as N-isopropylacrylamide (NIPAM) gives the hydrogel thermo-responsive behavior. Copolymerization of groups such as poly(hydroxyethyl methacrylate-coacrylic acid) or poly(acrylamide-co-acrylic acid) for example can give a multi-responsive (temperature and pH responsive) hydrogel system opening up more possibilities.[18]

Molecular Imprinting in hydrogels has become a useful means to detect biological targets because memory of template molecules is created within the hydrogel. The memory is said to be due to orientation of chemical groups that can form a complexation (non-covalent interactions) with the template. Imprinting allows the organization of monomers in a conformation that supports complexation of the template at multiple points and is often accomplished with the use of aptamers as receptors.[16]

Due to the outlined versatility described above and the macromolecular memory by imprinting, MIP hydrogels have been a great advancement in the field of recognition. Progress in the field has been propelled by the Miyata group who has incorporated molecular complexes into hydrogels. Among the many stimuli-responsive hydrogels they have developed is an α-Fetoprotein (AFP) imprinted hydrogel. Lectins and antibodies that are specific to AFP were modified with polymerizable groups and copolymerized with the AFP target. This formed lectin-AFP-antibody complexes, thus enabling the lectins and antibodies to be arranged at favorable positions for the recognition of AFP. The imprinted complex allowed for the removal and

specific rebinding of the AFP which was not seen in non-imprinted hydrogels (did not contain AFP prior to polymerization).[19,20]

The Spivak research group has also been instrumental in developing simple bio-responsive networks by employing imprinted hydrogels. They successfully imprinted the proteins thrombin and PDGF-ββ in the form of capillary hydrogels for naked-eye detection.[21] Acrylamide (AM) was used as the functional monomer and methylene bisacrylamide (MBAM) as the crosslinker in addition to target specific aptamers. Their results showed limits of detection as low as femtomolar concentrations of target protein. This was attributed to complex interplay between the aptamers and protein supermolecular crosslinks (utilizing noncovalent interactions) and also to the reduction of excluded volume in their gels.

Additionally, the Spivak group imprinted the apple stem pitting virus (ASPS) to show that other templates could be identified. Instead of making the hydrogels in capillaries, a new method was developed for synthesizing and measuring the hydrogels; a double imprinting technique. The double imprinting included the imprinting of the target virus at the molecular scale and an additional imprinted pattern at the macromolecular scale that was obtained by polymerizing the hydrogel in a lithographic mold.[22] This created a diffraction-grating sensor where the shrinking of the hydrogel to ASPS could be measured by the change in the diffraction pattern with faster response times.

Employing the imprinted hydrogel technique, a microRNA target was of interest. MicroRNA's are short, naturally occurring noncoding RNA sequences. These miRNAs also control gene expression such as differentiation and proliferation. When overexpressed, some of these sequences can exhibit oncogenic properties causing tumor growth.[23-25] Among these mRNAs is mir21 (Figure 3.2 (a)), it is a 22 base pair sequence that has been linked to colon and

breast cancer among others. There has been a wide array of research since its discovery in 1993, including methods to suppress mir21 overexpression[26-29] and detection methods[30-32]. Northern blotting is the most common method used for detecting microRNA's; others include Surface Enhanced Raman Spectroscopy (SERS) and fluorophore based detection.[33-35] In the field of MIPs, RNA research is very sparse and few examples can be found. One example by Longo et al. imprinted Tri-O-acetyladenosine using zinc-phthalocyanine as one of their functional monomers.[36] However, this was for separations and not as a detector and was for a specific base pair unlike the goals here where a sequence is the target.

Figure 3.2 (green, top) RNA mir21 sequence (purple, bottom) DNA mir21 mimic sequence

As opposed to using RNA, DNA was desired as the target; RNA is expensive and more difficult to handle since it is easily degradable. Thus, to develop a proof of concept a matching DNA mir21 mimic was studied in exchange (Figure 3.2 (bottom)). The difference between the RNA and DNA sequence is the nucleic acids thymine in the place of uracil (Figure 3.2) thereby it is not difficult to create a mimic sequence from DNA in the place of RNA. DNA has been widely studied for use in analytical sensors because it is chemically and physically stable, biocompatible and modifiable. Hybridization and dehybridization can be controlled at varying temperature, given as the temperature at which the DNA is unpaired, known as the melting temperature (T_m, equation 3.1).[37] The melting temperature can be modified based on the salt concentration (M); the salt decreases the electrostatic repulsion between the phosphate groups along the backbone of the DNA strands effectively controlling the annealing of DNA. This is, of

course, also dependent on the Guanine and Cytosine content (G/C) of the strands since they provide the most hydrogen bonding, as compared to Thymine and Adenosine, and in turn create stronger bonds.

$$T_m = 16.6\text{logM} + 0.41\ (\text{G/C}) + 81.5 \qquad \text{Equation 3.1}$$

There have been several studies on DNA incorporated into hydrogels because of DNA's stability and capability of modifications.[38] Flexibility can be added to the sequence by linking an 18-atom hexa-ethyleneglycol spacer (Sp18, Figure 3.3 (a)) and has been used to facilitate facile rebinding of the aptamer functionalized hydrogel to the template molecule.[21,22] For the incorporation of DNA into a hydrogel network it can be modified with a phosphoramidite or acrydite (Figure 3.3 (b)) for covalent conjugation to the polymer backbones. Hydrogels can also be formed by the DNA strands themselves with the addition of DNA ligases, e.g. T4 DNA ligase, to create a physically crosslinked system.[39] In an example by Lin et al. the authors used two acrydite modified oligos co-polymerized with acrylamide and added in a third DNA strand that was used to crosslink the system.[40]

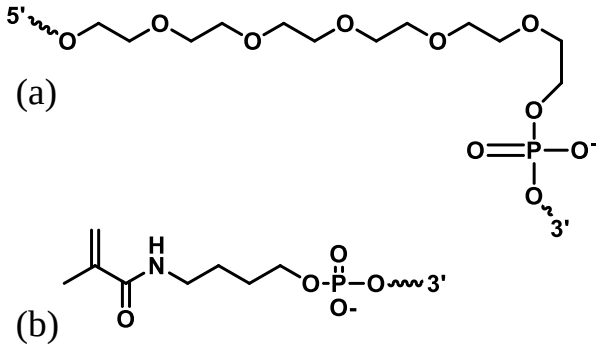

Figure 3.3. Functional modifies on the aptamers (a) acrydite (b) Sp18

Previous research in DNA sensors have been for larger target sequences with the shortest at 26 base pairs. This was achieved by using a quantum-dot-tagged bio-responsive hydrogel suspension array. When the target DNA strand was added to the hydrogel, the hydrogel shrank in

response causing a blue shift in the Bragg diffraction peak position which had a 10 nM limit of detection (LOD).[41] This example shows that it is possible to sense short DNA sequences, however several steps are required to synthesize the quantum-dot beads.

Other detection methods of DNA have utilized imprinted hydrogels. One example by Tierney et al. also deployed functionalized aptamers for a hydrogel attached to the end of an optical fiber for high resolution interferometric readout.[42] Their 35 base pair target sequences were detectable in the micromolar concentration range. Using gel electrophoresis Ogiso et al. created binding sites in the MIP gel that hindered the migration of their double stranded DNA target sequence (for 5 μM samples).[43]

The sensor designs that will be applied in this chapter will be the capillary imprinted hydrogels and the diffraction-grating sensors that were previously shown to perform well in the Spivak research group.[21,22] What distinguishes the sensor and application presented here apart from previous research is the size of the DNA target, the amount imprinted, the detectable limit of the target sequence and its later application towards detecting RNA sequences. Also of importance is the imprinting approaches where complimentary DNA aptamers are used to hybridize with the DNA target sequence prior and post polymerization.

The capillary hydrogels provide a simple sensor that directly measures the volume change by measuring the direct length changes of the gel associated with stimuli response such as the addition and removal of the target DNA mir21 mimic. Using the diffraction grating design is also advantageous in that the gratings are influenced by physical properties such as specific molecules by shrinking or swelling in response (i.e. addition and removal of a target), change in pH and temperature. These factors can, in turn, deform the grating structure making it possible to

observe the resulting shrinking/swelling responses by laser diffraction; in our case the addition and removal of the DNA mir21 target.

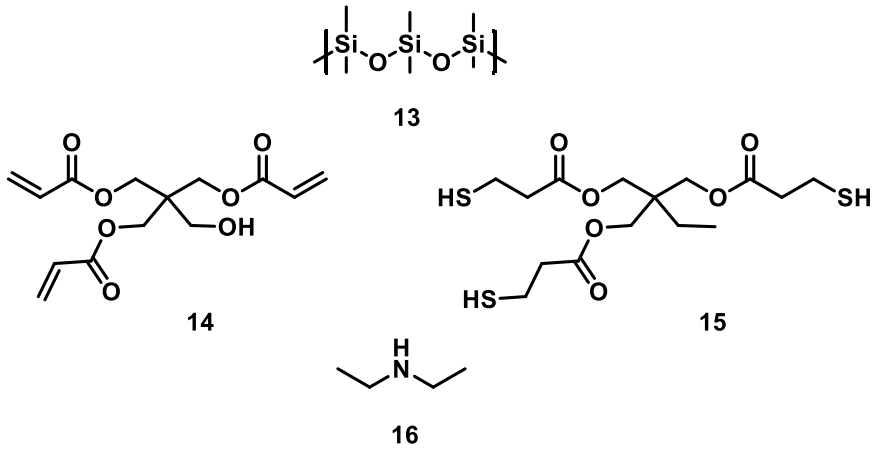

Figure 3.4 Structures of poly(dimethylsiloxane) (PDMS) 13, pentaerythritol triacrylate (PETA) 14, trimethylolpropane tris(3-mercaptopropionate) (TMPTMP) 15 and diethylamine 16.

An improved method for the diffraction-grating hydrogels will be discussed in detail (vide infra), the material used to transfer the grating pattern onto the hydrogel played an important role in creating the diffraction hydrogels. The most common material used as the hydrogel stamp or mold is poly(dimethylsilaxane) (PDMS, 13 Figure 3.4)[22,44-46] which produces a fine replica of the grating master to the mold; some of its useful properties include elastomeric nature, low cost of manufacturing and moldability to submicrometer features. The problem with this material lies in the transfer from the mold to the hydrogel due to PDMS's hydrophobicity making the introduction of aqueous solutions difficult in cases like microfluidics and in this case hydrogel patterning. Bounds et al. introduced an alternative in the form of thiol-acrylate materials.[47] Using pentaerythritol triacrylate (PETA) 14 and trimethylolpropane tris(3-mercaptopropionate) (TMPTMP) 15 that was catalyzed by diethylamine 16, they were able to fabricate stable hydrophilic microfluidic devices. Because of the success seen by this application, new diffraction-grating gels were made using the thiol-acrylate composite as the mold.

3.2 Results and Discussion of Capillary DNA mir21 Imprinted Hydrogels

Research focusing on imprinting hydrogels in the Spivak research group has been successful which lead us to focus on new avenues of sensors for various bio-macromolecule targets; the new target of interest was a mir21 DNA mimic. The hydrogels were imprinted in capillaries and the basic hydrogel preparation and synthesis can be seen in Figure 3.5 and previously in Figure 3.2 (b). The DNA target in Table 3.1 entry 1 is a short 22-mer sequence and its biomimetic receptors are the two 11 base pair aptamers (entries 2 and 3) that are complimentary to the DNA mimic.

Table 3.1 The sequences for the DNA mir21 mimic target and its complimentary aptamers

Reference Name	Entry	DNA sequence including modifications
DNA mir21 mimic	1	5’ – TAG CTT ATC AGA CTG ATG TTG A – 3’
Aptamer 1	2	5’ - /5Acryd /iSp18/ CTG ATA AGC TA – 3’
Aptamer 2	3	5’ - /5Acryd /iSp18/ TCA ACA TCA GT – 3’

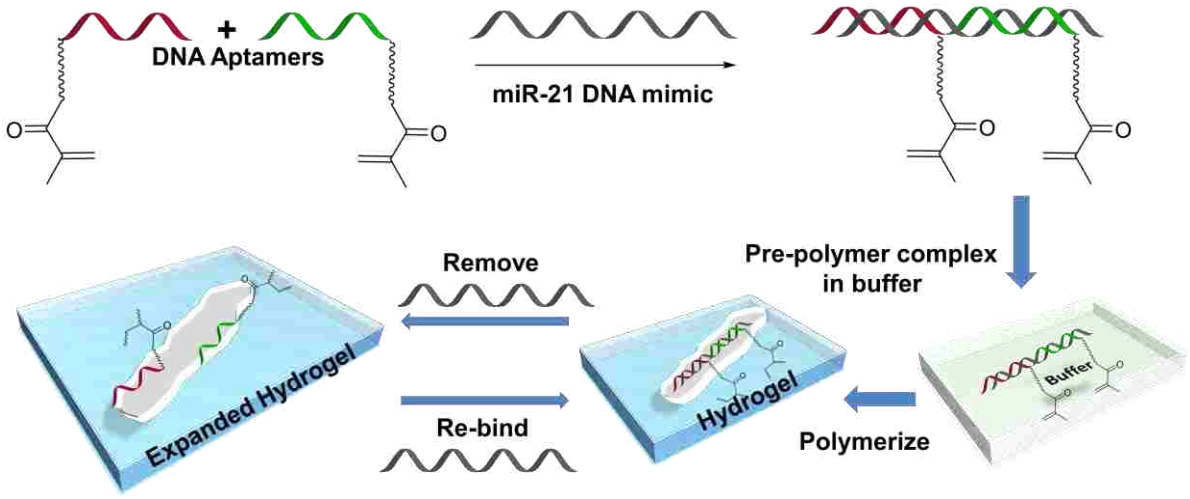

Figure 3.5 Illustration of binding of aptamer 1 and 2 to the DNA target, polymerization and response of DNA removal and rebinding to the polymerized hydrogel.

As listed in Table 3.1 both aptamers are modified at the 5’ end. Nucleotides hybridize from opposing ends, because of this it was imperative to verify that the position of the modifiers would not hinder the hybridization between the DNA mir21 target and aptamer 1 (as seen in Figure 3.5). To confirm that the modifications did not disrupt binding of the DNA complexes, a gel electrophoresis was used to verify that the DNA mir21 target and aptamers hybridize.

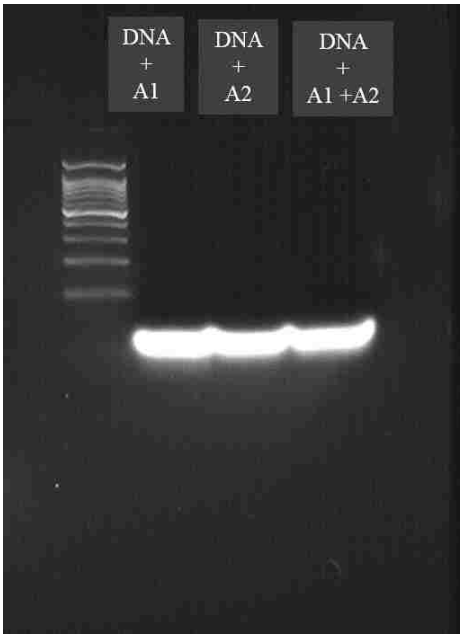

Figure 3.6 Agarose gel results for: the ethidium bromide (lane 1), DNA mir21 mimic with A1 (lane 2), A2 (lane 3) and A1 + A2 (lane 4).

The binding of aptamer 1 to the DNA mir21 target, aptamer 2 to the DNA mir21 target, and both aptamers with DNA mir21 target in solution was tested on an agarose gel (Figure 3.6) which was used to observe the change in base pairs by bands in the gel. The hybridization was tested by applying a current to the agarose gel with the DNA added to the wells. The phosphate groups along the DNA backbone are negatively charged and migrate to the positively charged anode. If the DNA was hybridized, one single band would be observed and if they were not there would be multiple bands for each sequence. Ethidium bromide was placed on the far left of the agarose gel as a reference to the base pairs traveling along the current; the shorter the sequence

the further the samples travel with the current and vice versa for longer strands. As seen in Figure 3.6, only single bands were observed for DNA with each variation of aptamers verifying that the DNA target effectively hybridizes with its complimentary aptamers during pre-polymerization. Additionally, a 1:1 mole ratio of the DNA target and the aptamers was used during the electrophoresis experiment which justified the mole equivalents used for future experiments.

3.2.1 Various Hydrogel Imprints and their response to the DNA mir21 mimic target

After testing the successful annealing of the DNA target to its aptamers, various hydrogels were made incorporating those DNA components plus monomers (NIPAM and acrylamide, AM), crosslinker (methylene bisacrylamide, MBAA) and initiators (ammonium persulfate, APS and tetramethylethylenediamine, TEMED) starting with the formulation listed in Table 3.2 for a total volume of 120 μL with the addition of PBS (phosphate-buffered saline). Based on past successes, the hydrogels were made in capillary tubes where the hydrogel's length change was measured in response to addition and removal of target DNA. All hydrogels were made in at least triplicates. The change in hydrogel length was evaluated as the percent shrinkage (equation 3.2) where the original length in the 0.05 M NaCl preparative solution is given as d_0 and the new length in response to the target analyte is denoted as d.

$$\%\, Shrinkage = \frac{d_0 - d}{d_0} x100 \qquad \text{Equation 3.2}$$

The distance between each meniscus of the capillary hydrogel was measured by a magnifying glass equipped with a ruler. The lengths measured are of the hydrogel with preparative 0.05 M NaCl to the maximum shrinkage with subsequent additions of 12 nM DNA mir21 target. Controlled hydrogels were made using the general formulation in Table 3.2;

adjusted accordingly for the non-imprinted hydrogel (NIP), polymerization without aptamers, and those polymerized with single aptamers.

Table 3.2 Formulation for DNA mir-21 mimic Imprinted Hydrogel

Reagent	MW (g/mol)	Mole equiv. of reagents	Mass of reagents used (mg)	Reagent concn. (mol/L)
DNA mir21 mimic	6764.5	1	0.017	2.1×10^{-5}
Aptamer 1	3931.8	1	0.087	2.1×10^{-5}
Aptamer 2	3891.7	1	0.086	2.1×10^{-5}
MBAM	154.17	390	0.15	8.3×10^{-3}
NIPAM/AM	113.16/71.08	80500	26/17	2.0

3.2.1.1 Various Formulations for Capillary Hydrogels

Table 3.3 Optimization of Capillary Hydrogels Performance via Concentration of Prepolymer Complex and Crosslinker Concentration for Maximum Volume Response

Entry	Ratio (MBAA:DNA complex)	% shrinkage response to DNA mir21 mimic
F1	390:1	5.7 ± 1.8
F2	267:1	1.9 ± 0.30
F3	203:1	1.1 ± 0.54
F4	320:1	1.2 ± 0.40

To optimize the hydrogel response, the original formulation from Table 3.2 (seen also in Table 3.3 entry F1) was adjusted; varying the volume of aptamers and target (also known as the complex) in the pre-polymerization mixture. It is beneficial to polymerize the least amount of

DNA as possible because the modified aptamers can be costly. Past examples showed a maximum response at the mole ratio of 483:1 for MBAA to A1-thrombin-A2 (complex).[21] For simplicity, just the amounts of crosslinker (MBAA) and DNA mir21 mimic are listed in Table 3.3; for entry F4 however, the amount of monomers and MBAA were also increased. The percent shrinkage results are also shown in Figure 3.7.

In Entry F2 the volume of DNA mir21 mimic and aptamers was increased to 1.5 times that of entry F1, this changed the MBAA:DNA ratio to 267:1 providing more reversible crosslinks. Increasing the ratio from 390 to 267, further increasing the amount of A1-DNA mir21-A2 complex, decreased the percent shrinkage to 1/3 the original response (entry F1).

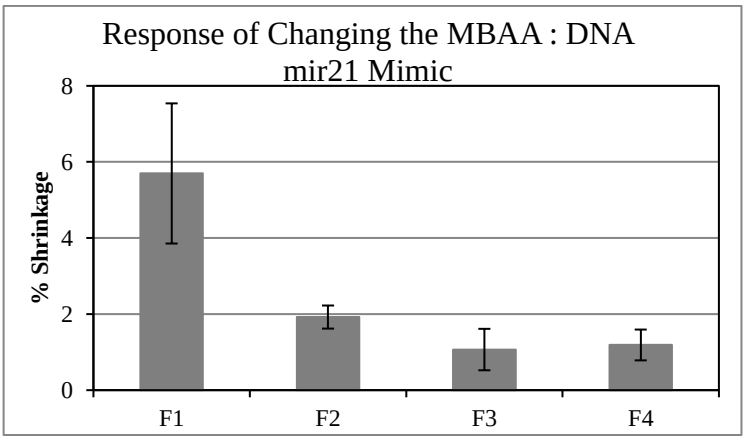

Figure 3.7 Percent shrinkage results with respect to changing the MBAA : DNA complex

Increasing the DNA complex by twice the amount of F1 (entry F3) during imprinting further decreased the response to the DNA mir21 target yielding 1.1 ± 0.54% shrinkage; indicating that as the complex is increased the response decreases in return. In Entry F4 the amounts of MBAA and monomers were increased by 1.2 times their original concentration in addition to increasing the DNA target and aptamers by 1.5 times giving a ratio of 320:1. This slight increase in crosslinking in comparison to F1 did not have an improvement on the response and resulted in 1.2% ± 0.40 shrinkage of the hydrogel. As compared to entry F2, having more

MBAA also decreases the response. The results for the formulation optimizations indicated that the best response was seen when polymerizing the least amount of complex (F1).

3.2.1.2 Controls: Changing the structural components

To verify the importance of incorporating both the aptamers and the DNA target into the imprinted complex, several controls were completed. These studies consisted of: single imprinted aptamers with the DNA mir21 (Figure 3.8), both aptamers and no DNA mir21 target, and the DNA mir21 target alone without aptamers. Each of these hydrogels was incubated with DNA mir21 mimic and the results are shown in Figure 3.9.

For this set of controls it was expected that, for the selective recognition of the DNA mir21 target, both aptamers are required to effectively hybridize the target and result in the largest response. Pre-complexation of both aptamers to the respective targets was previously shown by Bai et al. to be a key component in the response mechanisms for their hydrogels because multiple complexation points are required for imprinted polymers.[21,22] Hydrogels were polymerized with a single aptamer (aptamer 1 or 2) and the DNA mir21 target (Figure 3.8); all other components (monomers, crosslinker and initiators) remained the same. The results of the hydrogels are displayed in Figure 3.9 for response to the DNA mir21 target. Imprinting of aptamer 1 (A1) and the DNA mir21 target resulted in a significant loss of response; from 5.7% with both aptamers to 1.5 ± 0.94%. Similarly, including only apamter 2 (A2) and the DNA mir21 target resulting in a response of 1.7 ± 0.97%. Without both aptamers, there are reduced functional receptors present which is especially consequential due to the reduced amount of functional monomers (NIPAM/AM) within these imprinted hydrogels.

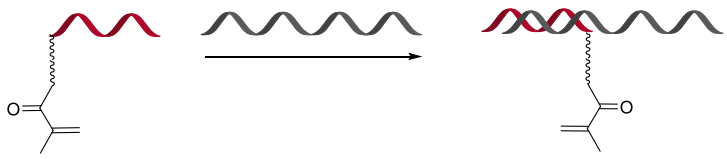

Figure 3.8 Hybridization representation of DNA mir21target plus aptamer 1 only.

To further verify the importance of incorporating the aptamers into the hydrogel for the DNA target recognition, a set of gels were made without aptamers imprinting only the target DNA. These hydrogels had no recognition elements and relied solely on the macromolecular memory formed during polymerization within the network. These hydrogels had a response of 0.66 ± 1.3% and in comparison to the single aptamer imprints show a decrease in recognition as the hydrogel loses both aptamer. Thus the hydrogels' response relies heavily on the hybridization of the DNA mir21 target to its complimentary aptamers and this is especially apparent in these control hydrogels where the response increases when polymerizing both aptamers. These results verified the significance of forming the full complex of A1-DNA mir21-A2 and removing a component of the complex had a negative effect on the responsiveness of the hydrogels.

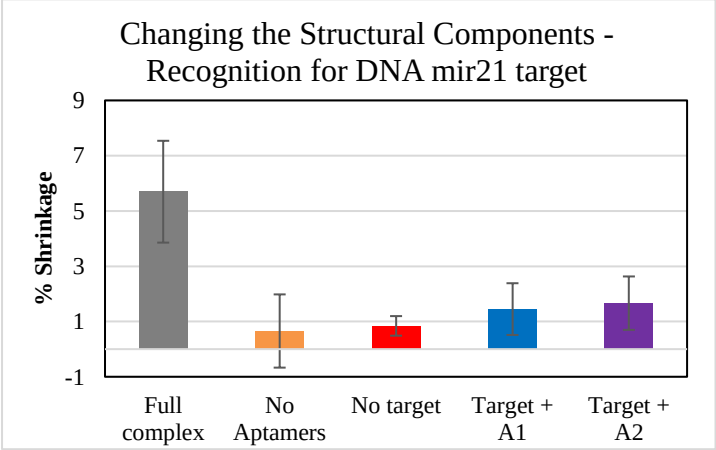

Figure 3.9 Shrinking response of hydrogels when polymerizing with the full A1-DNA-A2 complex, the target only, the aptamers only, the target and aptamer 1 and the target plus aptamers 2.

The next series of hydrogels were designed to study if it is necessary to have an imprinted system where both the aptamers and target are included in the polymerization. Hydrogels were polymerized without the DNA mir21 target, known as a non-imprinted polymer or "no target" as identified in Figure 3.9. This polymer still contained the aptamers within the hydrogel network and relied only on the hybridization of the aptamer/DNA complex formation post polymerization. In response to the DNA mir21, the hydrogels without a target gave a 0.84 ± 0.35% shrinkage. This is attributed to the random placement of aptamers when polymerized without the target instead of forming a pre-organized complex of A1-DNA mir21-A2; polymerizing the DNA target with the aptamers allows the aptamers to be arranged in a favorable orientation for rebinding of the DNA target.

3.2.1.3 Controls: Imprinting Different Target Sequences

A set of controls were made in the form of imprinting different target sequences as a follow-up to the aptamer controls in section 3.2.1.2. The studies provided a means of testing the selectivity of the aptamers and how that can affect the pre-complexing and resulting binding to DNA sequences. Several sequences were imprinted in the place of the DNA mir21 mimic (Table 3.4). Among these newly imprinted sequences are: anti-sequence, random, and a spacer.

Table 3.4 Sequences of the anti, random and spacer targets.

Reference Name	Entry	DNA sequence including modifications
Anti-sequence	1	5' – TCA ACA TCA GTC TGA TAA GCT A – 3'
Random sequence	2	5' – CGA TAG CAT CTG AGT CAC TTA G – 3'
5-spacer DNA mimic	3	5' – TAG CTT ATC AGT TTT TA CTG ATG TTG A – 3'

The referenced anti-sequence (Table 3.4 entry 1) is the full aptamer sequence, without the modified Sp18 and acrydite, arranged 5' to 3' and has five complementary pairs for each

aptamer. As highlighted in Figure 3.10 the anti-sequence contains five complimentary pairings in the middle of its sequence, providing a means of testing mismatched base pairs towards the ends of the sequence. As seen in Figure 3.11 when DNA mir21 sequence was added to the anti-imprinted hydrogel it gave a low response of 0.80 ± 0.13%. Although the anti-sequence is similar to the DNA mir21 mimic, any resulting complex or orientation of the aptamers formed during pre-polymerization is different than the full complimentary complex thus decreasing the response for the DNA mir21 target. Additionally, the anti-imprint was tested for its response to its imprinted "anti" sequence as seen in Figure 3.13. Incubating the imprinted sequence had a slightly larger response of 1.2 ± 0.49%; but without the aptamers forming a fully hybridized complex during pre-polymerization the aptamers will not be in a preferred orientation for rebinding. Examples of hybridization between non-complementary strands was shown by Ouldrige et. al. where the non-hybridized sections form different configurations.[48]

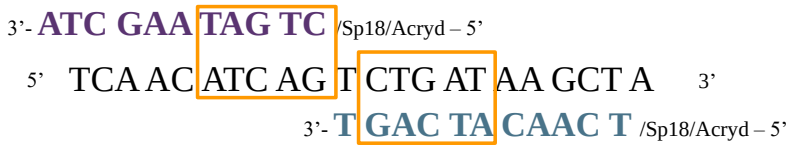

Figure 3.10 Aptamer interactions with the anti-sequence.

The next control was made by imprinting a sequence that has no complementarity to the aptamers, Table 3.4 entry 2, referred to as the "random" sequence. Figure 3.11 shows insignificant shrinking response to the DNA mir21 target of 0.20 ± 1.07%, even lower than that of the anti-imprinted polymer. Without any complementarity and resulting hybridization to the aptamers, the hydrogels displayed negligent response to the DNA mir-21 target. The random sequence was unable to form any complex with the aptamers which could have resulted in random placement of the aptamers, much like imprinting without a target sequence (Figure 3.9).

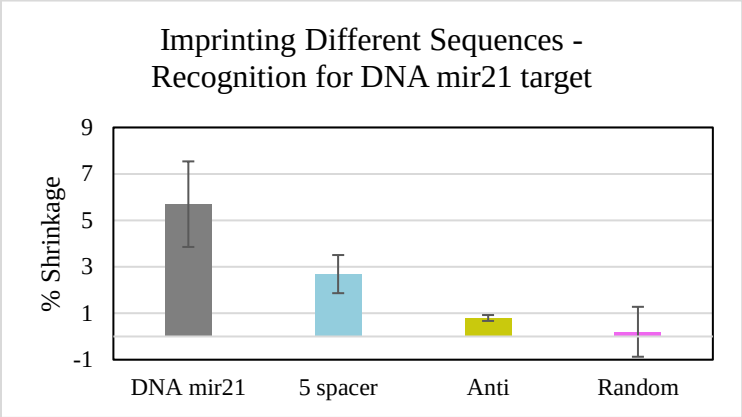

Figure 3.11 Hydrogels imprinted with various sequences and their response to the DNA mir21 target as compared to the DNA mir21 imprinted hydrogel.

The last sequence tested, 5-spacer (Figure 3.12), could hybridize to the aptamers at the ends of its sequence but had a short non-complimentary section in the middle made up of Thymine pairs. The objective here was to identify any non-specific binding that may occur with mismatched pairing towards the center of its sequence as opposed to the anti-sequence that had complementarity in the middle. The imprinting remained the same and the only difference was the imprinted target leaving an unhybridized section between the DNA mir21 spacer target (referenced as 5-spacer) and the aptamers (Figure 3.12).

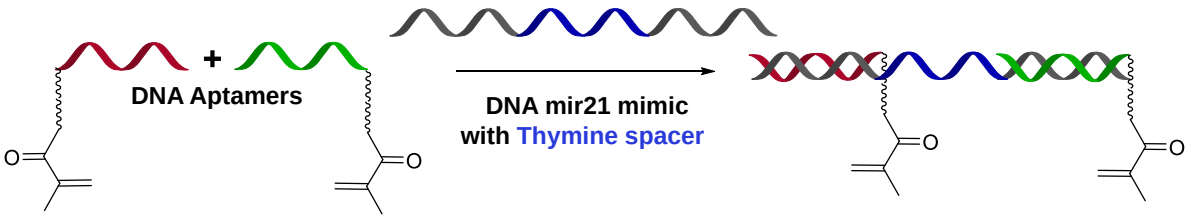

Figure 3.12 Spacer sequence hybridized with aptamers.

The result for the 5-spacer imprint also saw reduced recognition response with addition of the DNA mir21 mimic of 2.7 ± 0.82%. The reduction in response compared to the full complex imprint (5.7%) was not as significant as that of the anti-sequence (0.80%) or the

random (0.20%); however, it once again demonstrating how important it was to have full complementarity between the aptamers and the DNA sequence target.

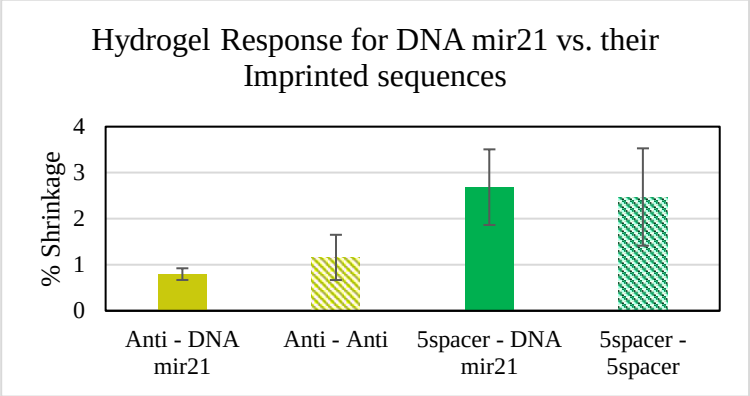

Figure 3.13 Response of the anti-imprinted hydrogel to the DNA mir21 target and the anti-sequence and the 5-spacer imprinted hydrogel response to the DNA mir21 target and the 5-spacer sequence.

An additional study was completed to understand more about the binding to the 5-spacer imprinted hydrogels (Figure 3.13). When the 5-spacer sequence was added to the 5-spacer imprinted hydrogels, it showed very little difference in recognition (2.5 ± 1.1% shrinkage) in comparison and also no improvement over the addition of the shorter DNA mir21 target. It is possible here that with the added spacing in the sequence that the hydrogel does not result in such a large collapse of the hydrogel. Also, because the DNA mir21 was not imprinted the aptamers are not arranged in the correct orientation thus decreasing likelihood for it to effectively bind to all of the aptamer pairs. Another explanation could be that the unhybridized section of thymine is single stranded and flexible which could cause the aptamers to bend or turn during the pre-polymerization in a different orientation than that of the fully hybridized DNA mir21 complex.

3.2.2 Investigating Selectivity in the DNA mir21 Imprinted Hydrogels

Once a successful imprinted hydrogel system was established it was crucial to study its selectivity towards its imprinted target versus similar sequences. As established by the above hydrogels imprinted for non-complimentary sequences that were tested for the DNA mir21 mimic which resulted in lack of response, there should also be no selectivity for other non-imprinted sequences in the DNA mir21 imprinted gel. To test this, three similar sequences were incubated: anti-sequence, 5 spacer and 20 spacer. The anti-sequence, as mentioned earlier, has some complementarity to the aptamers but has differing base pairs at the ends of the sequence. The spacers, however, have the exact same base pairs at the ends of their sequences but in the center of the sequence thymine was incorporated (five for the "5 spacer" and twenty for the "20 spacer").

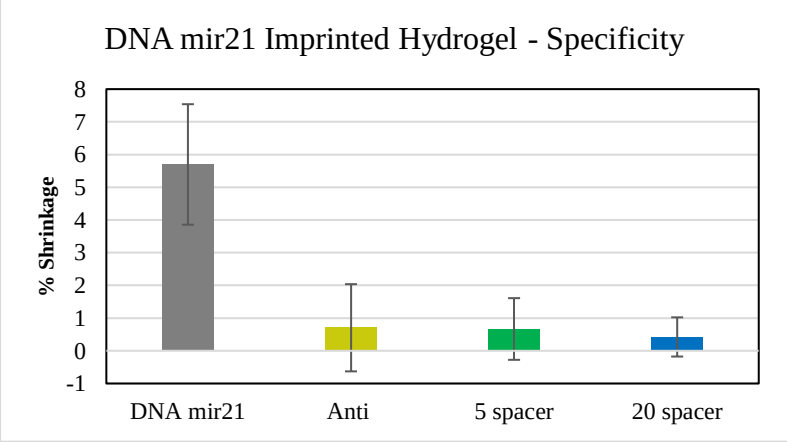

Figure 3.14 Investigating the selectivity of the DNA mir21 imprinted hydrogels with similar sequences.

The results for the DNA mir21 imprinted gel are displayed in Figure 3.14 for the various targets. When incubated with all three differing sequences there was less than 1% response by the hydrogels. This was expected based on the findings in the previous sections where the

hydrogels imprinted with similar sequences displayed very limited response to the DNA mir21 target.

Since the hydrogels do not have full complementary aptamers or the required pre-complexed binding, there should be no responsive recognition to these other sequences. In the case for the anti-sequence, it is possible for this piece to bind to the aptamers in a free solution with high enough salt concentration. However, the hydrogels were imprinted for the DNA mir21 target and the aptamers were arranged in the orientation to bind only the DNA mir21. Additionally, the hybridization of complementary sequences starts at the ends whereas the anti-sequence has complimentary base pairs in the middle of its sequence (Figure 3.10). According to Ouldridge et al. pairing of DNA strands start at the ends and then subsequently zipper or hybridize down the sequence.[48] With the spacer pieces, however, this is not the same issue as their complimentary base pairs are at the ends. The lack of response to these similar sequences is likely due to the pre-complexed binding, allowing for the aptamers to be arranged in a specific manner to the DNA mir21 imprinted target rather than the longer spacer sequences that contain non-interactive base pairs that do not hybridize to the aptamers.

3.3 Results and Discussion of Diffraction-Grating for DNA mir21 Imprinted Hydrogels

Based on the results shown by Bai et al. it was of interest to replicate the design of the Molecularly Imprinted Polymer Gel Laser Diffraction Sensor (MIP-GLaDiS) because they were able to show specific binding and recognition for the ASPV target.[22] Same as the capillaries a new target was evaulated, mir21, which has not been explored for MIPs. The original design used a PDMS (poly(dimethysiloxane), 13) mold to transfer the diffraction pattern onto the hydrogel. However, when using PDMS mold for the DNA mir21 hydrogels it would result in difficult reproducibility of the pattern from the mold to the hydrogel. PDMS has a hydrophobic

surface that expresses a water contact angle of about 105°C. An alternative to PDMS is made from a two part system of amine-catalyzed thiol-acrylate (TA) in the same manner as the PDMS (Figure 3.15). The TA system was prepared by the Pojman group where they used pentaerythritol triacrylate (PETA, 14) and trimethylolpropane tris(3-mercaptopropionate) (TMPTMP, 15) via a Michael Addition reaction using diethylamine (16) as the catalyst.[47] The large advantage of the TA as opposed to the PDMS material is that it is hydrophilic with a smaller water contact angle of 60°C which allows the aqueous hydrogel solution to enter into the patterned channels in TA's mold which resulted in a desirable visible pattern (Figure 3.16 (b)) on the hydrogel's surface. This is the same rationale for using TA in microfluidic devices because the TA composites produce stable hydrophilic surfaces.[47]

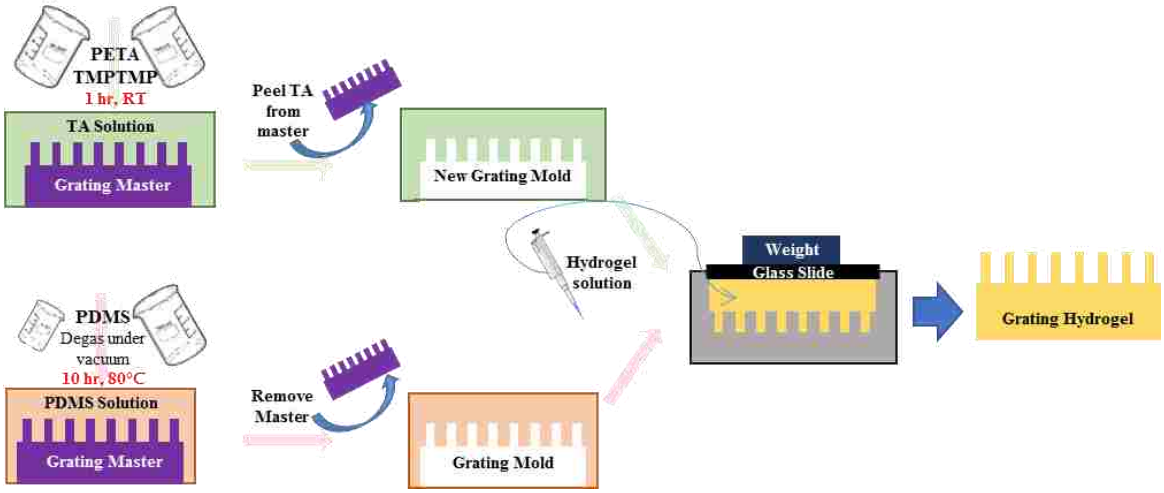

Figure 3.15 New mold designs for MIP-GLaDiS using TA versus PDMS

In addition to more precise molding, the new intermediary mold system was advantageous because it decreases the time between creation of the grating mold to the finished gel product resulting in faster processing as displayed in Figure 3.15. For the two part PDMS mold, a 10:1 mixture of elastomer base to curing agent is used and requires 10 hours for the solution to cure at 80°C. The T.A. mold uses a 1:1 ratio of PETA to TMPTMP and requires one

hour at room temperature for the mold to cure. After removing the master, the hydrogel solution can be added; however, the time required for the hydrogel solution to stay in each of the mold composites also differs on the amount of time needed for adequate transfer of the pattern to the hydrogel. When using a PDMS mold, the hydrogel solutions have to sit in the mold, clamped tightly, for over 72 hours for the gel to adopt the pattern (as previously determined by Bai) and in most cases the pattern does not transfer fully from the starting PDMS mold. However, using the TA composite mold the hydrogel solution only needs to remain in the mold for 12 hours or less, cutting the time dramatically. It should also be noted that the pattern on the hydrogel from the TA mold is a very good replica of the mold's grating pattern (Figure 3.16 (a)) and Figure 3.16 (b) shows the visible pattern on the hydrogel's surface.

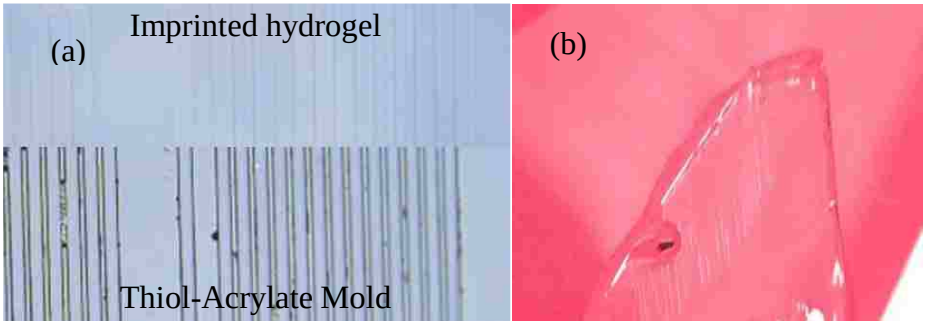

Figure 3.16 (a) Diffraction pattern of the imprinted hydrogel (top) as compared to the thiol-acrylate mold (bottom) (b) picture of the visible pattern on the surface of the hydrogel.

The change in the diffraction pattern channels by microscope images in addition to the change in distance in the resulting diffraction by the laser pointer can be seen. Figure 3.17 (a) shows how the distance between the channels shrinks in response to the rebinding of DNA mir21 to the hydrogel and the resulting swelling as seen by the larger distance in the channels. The change in the diffraction pattern distances can be seen Figure 3.17 (b) where the hydrogel with DNA mir21 results in a greater distance between the pattern and when the DNA mir21 is removed the distance in the diffraction pattern grows smaller. The inverse relationship between

the pattern distance and the hydrogel shrinking and swelling can be explained by application of the equations below:[22]

$$\theta = sin^{-1}(\frac{\lambda}{d}) \qquad \text{Equation 3.3}$$

$$\theta = tan^{-1}(\frac{D}{h}) \qquad \text{Equation 3.4}$$

$$D = h\ tan\left[sin^{-1}(\frac{\lambda}{d})\right] \qquad \text{Equation 3.5}$$

The distance in the diffraction pattern (d) can give the angle of diffraction (θ) for the transmitted laser light (Equation 3.3, λ is the wavelength of the laser source and is 532 nm for the green laser pointer used herein). As a result, when θ becomes larger the distance between the diffraction patterns becomes smaller. The distance between two adjacent projected laser points (D) can be determined by θ seen in Equation 3.4 which is also dependent on the height (h) of the laser source. When the two equations are combined (equation 3.5) it gives an inversely proportional relationship between the distance (D) and the grating period; meaning as the hydrogel swells, the distance between the laser points decreases (Figure 3.17 (b)).

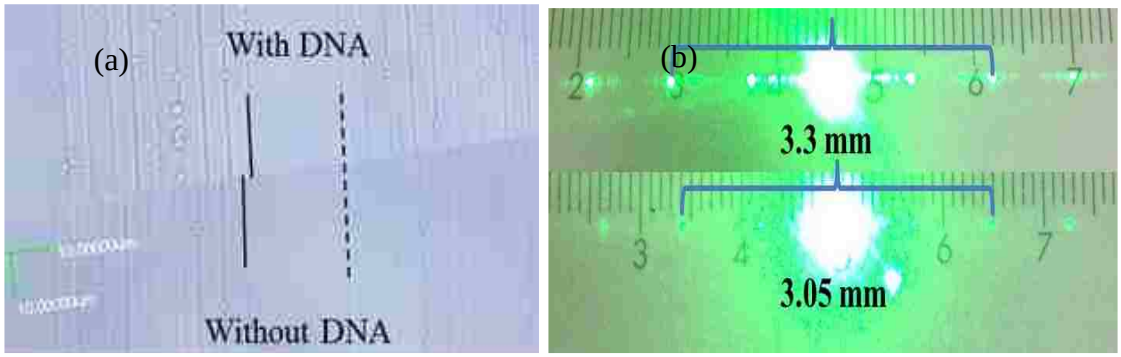

Figure 3.17 (a) Microscope images of the DNA mir21 imprinted grating gels in response to the addition (top) and removal (bottom) of DNA mir21 target. (b) Resulting diffraction pattern with DNA mir21 in the top image and the hydrogel without DNA mir21.

3.3.1 Optimization of Parameters for the Diffraction Gratings

Similar to the capillary hydrogels above (section 3.2), optimization of the formulation for the diffraction grating hydrogels was also explored. Different from the capillaries however, the amount of MBAA and monomers were decreased instead of the DNA complex. The formulation changes were prompted from previous work by Bai et al. who found that the grating hydrogels with the largest response were those made with lower monomer and crosslinker.[22] The mole ratios can be observed in Table 3.5 where the crosslinker, monomers and DNA complex are listed with the resulting percent shrinkage to the DNA mir21 target (also presented in Figure 3.18). The percent shrinkage of the gels was calculated using Equation 3.1, similarly to the capillary gels.

Table 3.5 Formulation changes for the DNA mir21 mimic diffraction grating hydrogels via monomer and crosslinker concentration and the maximum volume response.

Entry	Ratio (MBAA:Monomers:DNA)	% shrinkage response to DNA mir21 mimic
G1	390:93000:1	3.5 ± 0.53
G2	260:78000:1	4.2 ± 0.40
G3	208:68000:1	2.9 ± 0.46

Using the same formulation as the capillary hydrogels (F1 in Table 3.3), the grating hydrogels displayed a 3.5 ± 0.53% response. Upon lowering the amount of monomers and crosslinker by 1.2 times for G2, the best response of 4.2 ± 0.40% to the target was observed without losing the orientation of the A1-DNA mir21-A2 complex. Further decreasing the monomers by 1.5 and the MBAA by 1.9 did not improve the response (2.9 ± 0.46%) and so the formulation of G2 was used for further experiments. The decrease in response by G3 in

comparison to G2 could be because the system was not crosslinked enough, dissociating the orientation of the receptors (aptamers) and hindering the complexation of both the aptamers with the DNA mir21 target.

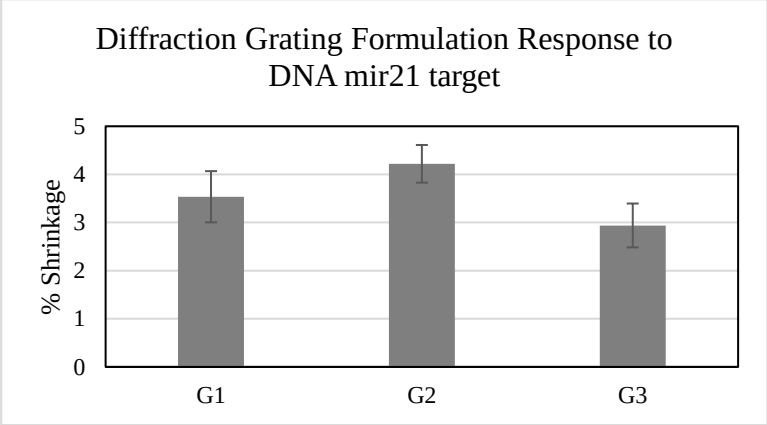

Figure 3.18 Formulation optimization for the diffraction grading hydrogels and their response to the DNA mir21 target

In addition to the initial response tests for the grating hydrogels, a study was done to test the reversible nature of these systems. Figure 3.19 shows the response of G2 over three cycles of adding the DNA mir21 target, removing it with water and the re-addition of the DNA target. The reversible behavior of the hydrogel shows the stability of the system over multiple cycles with an average response of 4.4 ± 0.055 %.

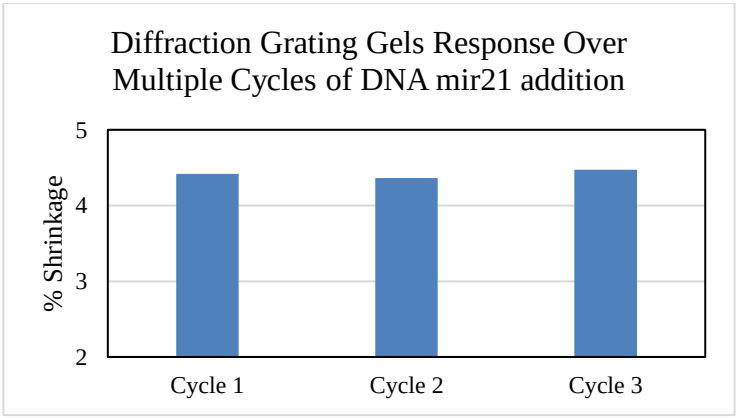

Figure 3.19 Reversible volume change of the diffraction grating hydrogel, G2, over multiple cycles

3.3.2 Controls: Diffraction Grating Hydrogels Investigation of Aptamers and Target

Similar to the treatment of the capillary hydrogels in section 3.2, several controls were made to ensure that the grating hydrogels also required the polymerization of the complexed A1-DNA mir21-A2. The control hydrogels made were polymerized with: a single aptamer and the target, no aptamers (target only), and both the aptamers without the target. These hydrogels were tested for the response to the DNA mir21 target and their results are displayed in Figure 3.20.

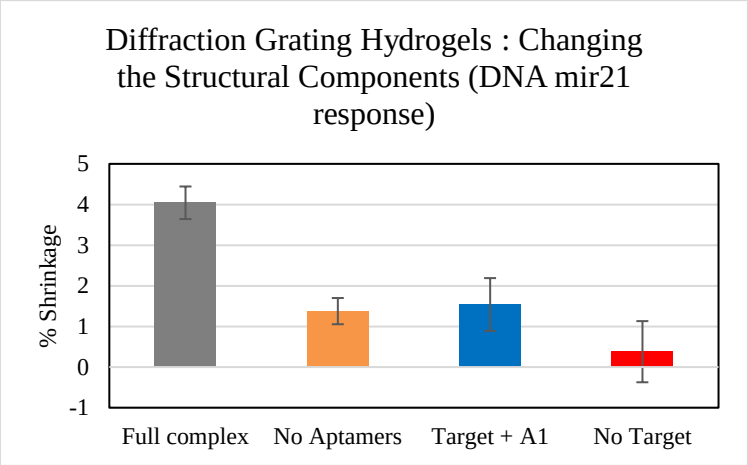

Figure 3.20 DNA mir21 response upon altering the aptamers and DNA mir21 target for the diffraction grating hydrogels.

As previously shown for the capillary hydrogels, it is imperative to incorporate all components of the A1-DNA mir21-A2 complex. The response seen for the hydrogel that included a single aptamer resulted in 1.5 ± 0.65 % shrinkage and the response decreased slightly more without any aptamers present (1.4 ± 0.32 %). Hydrogels imprinted without the DNA mir21 target also resulted in a very low response of 0.38 ± 0.75 %. These results reiterated the importance of having the full A1-DNA mir21-A2 complex prior to polymerization. Removing a component within the complex significantly decreases the shrinking response of the hydrogels where the rebinding of the DNA mir21 target is dependent on the hybridization to both of the aptamers. Unlike traditional imprinted polymers, like those used for separations, the light

crosslinking and low amount of the functional monomers of the MIP hydrogels relies on the aptamers as receptors for the selective rebinding of the DNA mir21 target provided by the pre-organization of the aptamers and DNA target prior to polymerization.

3.4 Discussion for the Shrinking Response of the DNA mir21 Hydrogels

Past examples of DNA hydrogels were structured differently than our system thus the mechanisms of the response to their target were different than ours. In an example by Murakami et. al. they developed DNA crosslinked hydrogels, where the aptamers are crosslinked as part of the hydrogel backbone, that shrank in response to addition of their target sequence because of the change in chain length from the longer single stranded DNA to the shorter double stranded DNA when the complimentary sequence was added.[49] The length change is due to the flexible single stranded DNA being hybridized with a complimentary single stranded DNA forming a rigid double helix.

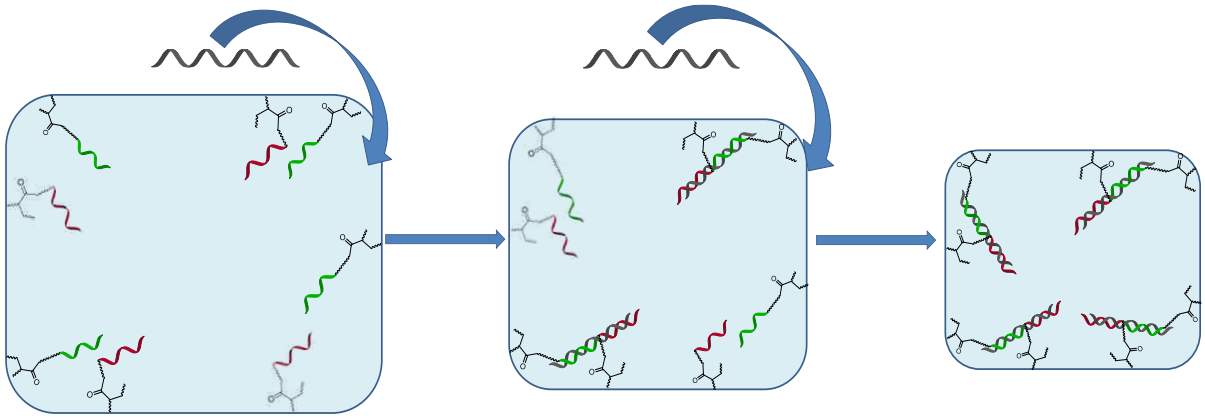

Scheme 3.1 Shrinking illustration of DNA mir21 imprinted hydrogels in response to multiple additions of DNA mir21 target. As more DNA mir21 solution is added, the hydrogels additionally shrinks possibly due to the aptamers becoming closer to the optimal orientation for DNA mir21 binding.

Based on the results from sections 3.2.1.2 and 3.3.2, we know that the shrinking response for our hydrogel system was very dependent on having both of the aptamers which act as the functional receptors in the hydrogel network which lead us to believe that the hybridization of

the complex causes the shrinking response for these DNA imprinted hydrogels. Unlike the above example[49], however, the aptamers are not crosslinked to the hydrogel network on both ends and thus are not directly part of the crosslinking mechanism. The system we used, instead, relied heavily on the imprinting effect of arranging the aptamers in cooperative orientation for the rebinding of the DNA target. A proposed explanation of the shrinking is depicted in Scheme 3.1 where there could be aptamers (which are crosslinked at the 5' end) arranged towards the corners of the hydrogel allowing those aptamers and DNA target to easily bind with the first addition of the DNA mir21 target. The theory of cornered aptamer groups is assuming the hydrogels are made up of multiple layers of cubes within our network. Once the corners hybridize this could cause the hydrogel to shrink slightly allowing the next set of aptamers to bind to the target when more is added because they are in a closer orientation causing the hydrogel to collapse more as a result of each addition of DNA mir21 target. The shrinking response could be a result of percolation which would account for the larger than expected response of our hydrogels as compared to the above examples where the aptamers are fully crosslinked within the hydrogel. Percolation theory can be described where the solute molecules connect by pores that can diffuse.[50]

For both the capillaries and the grating hydrogels, additional shrinking was observed each time more of the DNA mir21 solution was added to the hydrogels which is consistent with the theory. Data presented in Figure 3.21 shows that there is a shrinking response of our hydrogels each time more of the DNA mir21 target was added for the grating diffraction hydrogels and this effect was also seen for the capillary hydrogels (data not shown). After a certain amount of DNA mir21 is added to the hydrogels, the hydrogel stops shrinking possibly due to reaching a saturation point. The hydrogel is imprinted for a micromolar amount of the complex so once this

amount is reached within the hydrogel there should be no cause for the DNA mir21 target to rebind above that concentration.

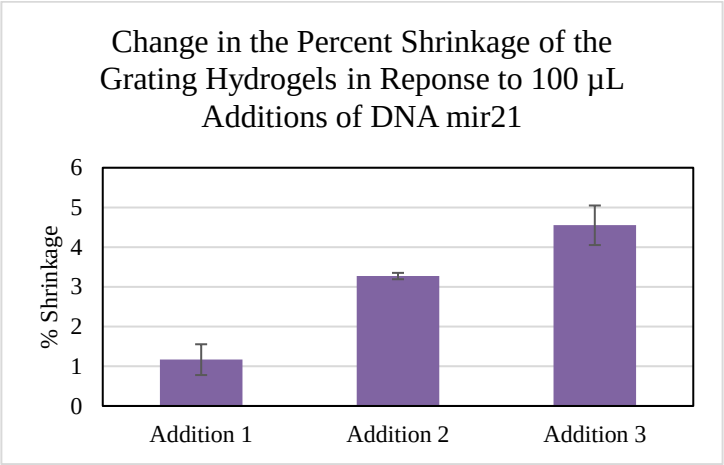

Figure 3.21 Subsequent Shrinking Response of the Grating Hydrogels as more DNA mir21 solution is added.

3.5 Conclusions

A new hydrogel sensor system was developed for a mir21 DNA mimic. The capillary imprinted hydrogel system was optimized giving an average response of 5.7 % shrinkage of the gel. Removing any of the components, such as the aptamers or the DNA mir21 target during the polymerization has a negative effect on the response of the gel, indicating that a fully complexed system is required (A1-DNA mir21-A2). When imprinting other sequences, such as the random or anti-sequence, the hydrogel had no response for the DNA mir21 mimic owing to the importance of the imprinted complex and the fully complimentary aptamers for recognition. Also of importance was the selectivity of the DNA mir21 imprinted gels that were only responsive to the DNA mir21 target, even with a similar sequence like the 5 spacer that had the same complimentary sequences with the addition of five thymine nucleotides as spacers in the middle of its sequence.

The second sensor system studied was the MIP-GLaDiS sensors that had a micro- and macro-imprint. A new approach to the hydrogel stamping was employed using PETA and TMPTMP (TA) in the place of PDMS. The TA composite material is more hydrophilic which allowed for the effective and reproducible transfer of the pattern on the TA mold to the gel. The diffraction hydrogels displayed similar results as the capillary hydrogels was a 4.2 % response to the DNA mir21 target. The imprinted complex was shown to be imperative to the gels response to the DNA mir21 target which supports the necessity for an imprinted system. The swelling and shrinking response of the diffraction hydrogel can be seen by the change in the diffraction pattern relative to the addition and removal of the DNA mir21 target and could be used for multiple cycles.

Possible explanations for the shrinking response of the hydrogel to the DNA mir21 target were believed to be caused by initial hybridization of cornered aptamers in closer proximity to bind the DNA target. As additional DNA mir21 was added the hydrogels subsequently shrank more in response. Both the capillary and diffraction grating gels were proven to be successful for their intended target and displayed the importance of imprinting with a short DNA sequence. These imprinted hydrogels also match detectable concentrations of other DNA detectors with a known detection in the nanomolar range.[42,43,49]

3.6 Future Work

This system needs to, most importantly, be tested for mir21 in place of its DNA mimic to ensure that the system works for the desired target. Additionally, isotherm studies are necessary to determine the LOD for these imprinted hydrogels. Also, a sequence with just one or more mismatches should also be tested to identify the exact selectivity of our hydrogels.

Having an additional detection mechanism was of interest, especially to further the sensitivity of the hydrogels. One way to achieve this is to incorporate a fluorescent aspect into the hydrogel. Nile blue is a fluorescent dye typically used in gel electrophoresis as a stain to visualize DNA. Nile blue is among the phenoxazine family of dyes, which are known to have high fluorescence quantum yields and fluorescence at long wavelengths.

The Nile blue can be incorporated into the hydrogel network by adding a polymerizable group such as acrylamide or methacrylamide, similar to the aptamers (Scheme 3.1). Because the workup has been completed, the experimental section outlines the synthesis to modify Nile blue with methacrylamide. Although there was not adequate time to incorporate this dye into the sensor it at the current time it is still a desirable addition to improve the measuring response.

3.7 Experimental Work

Capillary Hydrogel preparations and polymerization

The hydrogel preparations first starts with making a Phophate Buffer Saline (PBS pH = 7.4) solution which is then used to make the solutions of ammonium persulfate (APS), N,N'-methylenebisacrylamide (MBAM, 6.6 x 10^{-2} M) and the monomers N-isopropylacrylamide/acrylamide (NIPAM/AM 7.8 M). The corresponding amounts of DNA mir-21 mimic and aptamers are added together in a microcentrifuge tube with half of the PBS solutions (30 µL) (Table 3.2) and placed in a 90°C water bath for two minutes. The DNA solution was then allowed to slowly cool to room temperature while remaining in the water bath to anneal and the remaining PBS (30 µL), APS (6.3 µL, 10 wt% in PBS buffer), MBAM (1 wt% in PBS buffer) and monomers solutions were added. Purging of the solution with nitrogen followed and TEMED (0.6 µL) was added last. Once the TEMED was placed into the tube, the solution was quickly vortexed and a capillary with dimensions 1.7mm inner diameter and 10cm

in length was dipped into the tube. The capillary pulled the hydrogel solutions up via capillary action, was sealed with parafilm and allowed to sit to complete polymerization. Prior to use, the capillary tubes were cleaned using piranha solution, rinsed well with deionized water and dried in a low temperature oven to remove any remaining moisture. All capillaries were done in triplicates.

Grating Hydrogel solution prep and measurements

The TA grating molds were made by Michael Tullier in the Pojman research team and followed the procedure published.[47] The diethylamine (16.1 mol %) was added to the PETA to form the trifunctional acrylate and the TMPTMP was then added in a 1:1 mole ratio (thiol to acrylate functional groups). The TA was added over the grating master with gratings 5 μm of negative photoresist SU-8 (purchased from MicroChem Corp.) on a silicon wafer. The masters used were cut and sized to 1.0 cm^2 and a plastic backing was added to add depth to the resulting grating molds.

The new grating molds were rinsed with deionized water and dried with nitrogen and the hydrogel solution (prepared the same as the above capillary solution) was added into the well of the grating mold using a micropipette. A small glass slide was placed on top of the hydrogel solution, clamped and allowed to sit overnight. After approximately 12 hours the mold, hydrogel and glass slide were placed into a small pitre dish with water. After about 30 minutes the glass slide was removed and the hydrogel was cut from the mold.

Measurements were performed by placing the hydrogel onto a glass slide, another smaller glass slide was placed on top and the hydrogel was measured using a green laser pointer (532 nm). A pink piece of paper was placed on the floor of the fume hood in which the laser apparatus was set up and a clear yellow diffraction pattern was observed. Because the diffraction grating

gels were shown to be stable after multiple cycles (Figure 3.19) the gels were made in singles or duplicates and the percent shrinkage was determined from three separate cycles between one or two hydrogels.

Nile Blue Methacrylamide synthesis from Nile Blue A

The synthesis of the Nile Blue methacrylamide (NBM) follows a published procedure (Scheme 3.2). Nile Blue A (NBA) (1 g, 2.74 mmol) is weighed into a 50 mL round bottom flask with a stir bar. This was followed by addition of DCM (50 mL) and trimethylamine (1.2 mL, 8.6 mmol) which garnered a red/ maroon solution, then placed under nitrogen and an ice-bath. A solution of DCM (10 mL), methacrylic anhydride (0.6 mL, 4 mmol) and DMAP (20 mg, 0.175 mmol) were added next and the solution was allowed to reach room temperature.

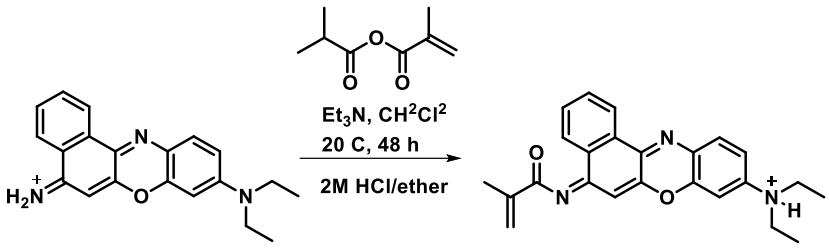

Scheme 3.2 Nile blue methacrylamide synthesis from Nile Blue A

After stirring for 22 hours, additional methacrylic anhydride (0.22 mL, 1.48 mmol) and triethyamine (0.4 mL, 2.86 mmol) were added and left to stir for an additional 26 hours. The solid was then washed with water and filtered leaving behind blue crystals. From there, ether was added yielding a dark red solution and 2 M HCl in diethyl ether was added which then turned the solution dark blue. The round bottom was cooled to -10°C and left to stir over night and the temperature was left to gradual warm to room temperature. The following day, after rotovaping the ether down, the crystals were filtered and washed with water. The remaining solid was dried in a vacuum oven at 25 °C yielding blue crystals.

3.8 References

(1) Juers, D. H.; Matthews, B. W.; Huber, R. E. LacZ β-galactosidase: Structure and function of an enzyme of historical and molecular biological importance. *Protein Sci.* **2012**, *21*, 1792-1807.

(2) Raap, J.; Kerling, K. E. T.; Vreeman, H. J.; Visser, S. Peptide substrates for chymosin (rennin): conformational studies of κ-casein and some κ-casein-related oligopeptides by circular dichroism and secondary structure prediction. *Arch. Biochem. Biophys.* **1983**, *221*, 117-124.

(3) Drolet, D. W.; Jenison, R. D.; Smith, D. E.; Pratt, D.; Hicke, B. J. A high throughput platform for systematic evolution of ligands by exponential enrichment (SELEX). *Comb. Chem. High Throughput Screening* **1999**, *2*, 271-278.

(4) Musheev, M. U.; Krylov, S. N. Selection of aptamers by systematic evolution of ligands by exponential enrichment: Addressing the polymerase chain reaction issue. *Anal. Chim. Acta* **2006**, *564*, 91-96.

(5) Sapsford, K. E.; Bradburne, C.; Delehanty, J. B.; Medintz, I. L. Sensors for detecting biological agents. *Mater. Today (Oxford, U. K.)* **2008**, *11*, 38-49.

(6) Homola, J. Surface plasmon resonance sensors for detection of chemical and biological species. *Chem. Rev. (Washington, DC, U. S.)* **2008**, *108*, 462-493.

(7) Hellio, D.; Djabourov, M. Physically and chemically crosslinked gelatin gels. *Macromol. Symp.* **2006**, *241*, 23-27.

(8) Maitra, J.; Shukla, V. K. Cross-linking in hydrogels - a review. *Am. J. Polym. Sci.* **2014**, *4*, 25-31, 27 pp.

(9) Buwalda, S. J.; Boere, K. W. M.; Dijkstra, P. J.; Feijen, J.; Vermonden, T.; Hennink, W. E. Hydrogels in a historical perspective: From simple networks to smart materials. *J. Controlled Release* **2014**, *190*, 254-273.

(10) Wichterle, O.; Lim, D. Hydrophilic Gels for Biological Use. *Nature* **1960**, *185*, 117-118.

(11) Jee, E.; Bansagi, T., Jr.; Taylor, A. F.; Pojman, J. A. Temporal Control of Gelation and Polymerization Fronts Driven by an Autocatalytic Enzyme Reaction. *Angew. Chem., Int. Ed.* **2016**, *55*, 2127-2131.

(12) Barron, V.; Killion, J. A.; Pilkington, L.; Burke, G.; Geever, L. M.; Lyons, J. G.; McCullagh, E.; Higginbotham, C. L. Development of chemically cross-linked hydrophilic-hydrophobic hydrogels for drug delivery applications. *Eur. Polym. J.* **2016**, *75*, 25-35.

(13) Jadhav, R. A review on hydrogel as drug delivery system. *World J. Pharm. Res.* **2015**, *4*, 578-599.

(14) White, E. M.; Yatvin, J.; Grubbs, J. B., III; Bilbrey, J. A.; Locklin, J. Advances in smart materials: Stimuli-responsive hydrogel thin films. *J. Polym. Sci., Part B: Polym. Phys.* **2013**, *51*, 1084-1099.

(15) Koetting, M. C.; Peters, J. T.; Steichen, S. D.; Peppas, N. A. Stimulus-responsive hydrogels: Theory, modern advances, and applications. *Materials Science and Engineering: R: Reports* **2015**, *93*, 1-49.

(16) Byrne, M. E.; Salian, V. Molecular imprinting within hydrogels II: Progress and analysis of the field. *Int. J. Pharm.* **2008**, *364*, 188-212.

(17) Schmaljohann, D. Thermo- and pH-responsive polymers in drug delivery. *Adv. Drug Delivery Rev.* **2006**, *58*, 1655-1670.

(18) Dong, L. C.; Hoffman, A. S. A novel approach for preparation of pH-sensitive hydrogels for enteric drug delivery. *J. Controlled Release* **1991**, *15*, 141-152.

(19) Miyata, T. Preparation of smart soft materials using molecular complexes. *Polym. J. (Tokyo, Jpn.)* **2010**, *42*, 277-289.

(20) Miyata, T.; Jige, M.; Nakaminami, T.; Uragami, T. Tumor marker-responsive behavior of gels prepared by biomolecular imprinting. *Proc. Natl. Acad. Sci. U. S. A.* **2006**, *103*, 1190-1193.

(21) Bai, W.; Gariano, N. A.; Spivak, D. A. Macromolecular Amplification of Binding Response in Superaptamer Hydrogels. *J. Am. Chem. Soc.* **2013**, *135*, 6977-6984.

(22) Bai, W.; Spivak, D. A. A Double-Imprinted Diffraction-Grating Sensor Based on a Virus-Responsive Super-Aptamer Hydrogel Derived from an Impure Extract. *Angew. Chem., Int. Ed.* **2014**, *53*, 2095-2098.

(23) Asangani, I. A.; Rasheed, S. A. K.; Nikolova, D. A.; Leupold, J. H.; Colburn, N. H.; Post, S.; Allgayer, H. MicroRNA-21 (miR-21) post-transcriptionally downregulates tumor suppressor Pdcd4 and stimulates invasion, intravasation and metastasis in colorectal cancer. *Oncogene* **2008**, *27*, 2128-2136.

(24) Campuzano, S.; Torrente-Rodriguez, R. M.; Lopez-Hernandez, E.; Conzuelo, F.; Granados, R.; Sanchez-Puelles, J. M.; Pingarron, J. M. Magnetobiosensors Based on Viral Protein p19 for MicroRNA Determination in Cancer Cells and Tissues. *Angew. Chem., Int. Ed.* **2014**, *53*, 6168-6171.

(25) Frankel, L. B.; Christoffersen, N. R.; Jacobsen, A.; Lindow, M.; Krogh, A.; Lund, A. H. Programmed Cell Death 4 (PDCD4) Is an Important Functional Target of the MicroRNA miR-21 in Breast Cancer Cells. *J. Biol. Chem.* **2008**, *283*, 1026-1033.

(26) Bose, D.; Nahar, S.; Rai, M. K.; Ray, A.; Chakraborty, K.; Maiti, S. Selective inhibition of miR-21 by phage display screened peptide. *Nucleic Acids Res.* **2015**, *43*, 4342-4352.

(27) Devulapally, R.; Sekar, T. V.; Paulmurugan, R. Formulation of Anti-miR-21 and 4-Hydroxytamoxifen Co-loaded Biodegradable Polymer Nanoparticles and Their Antiproliferative Effect on Breast Cancer Cells. *Mol. Pharmaceutics* **2015**, *12*, 2080-2092.

(28) Seeger, T.; Fischer, A.; Muhly-Reinholz, M.; Zeiher, A. M.; Dimmeler, S. Long-term inhibition of miR-21 leads to reduction of obesity in db/db mice. *Obesity* **2014**, *22*, 2352-2360.

(29) Zhou, X.; Li, Y.-J.; Gao, S.-Y.; Wang, X.-Z.; Wang, P.-Y.; Yan, Y.-F.; Xie, S.-Y.; Lv, C.-J. Sulindac has strong antifibrotic effects by suppressing STAT3-related miR-21. *J. Cell. Mol. Med.* **2015**, *19*, 1103-1113.

(30) Hao, N.; Li, X.-L.; Zhang, H.-R.; Xu, J.-J.; Chen, H.-Y. A highly sensitive ratiometric electrochemiluminescent biosensor for microRNA detection based on cyclic enzyme amplification and resonance energy transfer. *Chem. Commun. (Cambridge, U. K.)* **2014**, *50*, 14828-14830.

(31) Kilic, T.; Erdem, A.; Erac, Y.; Seydibeyoglu, M. O.; Okur, S.; Ozsoz, M. Electrochemical Detection of a Cancer Biomarker mir-21 in Cell Lysates Using Graphene Modified Sensors. *Electroanalysis* **2015**, *27*, 317-326.

(32) Park, J.; Yeo, J.-S. Colorimetric detection of microRNA miR-21 based on nanoplasmonic core-satellite assembly. *Chem. Commun. (Cambridge, U. K.)* **2014**, *50*, 1366-1368.

(33) Pall, G. S.; Hamilton, A. J. Improved northern blot method for enhanced detection of small RNA. *Nat. Protoc.* **2008**, *3*, 1077-1084, S1077/1071.

(34) Driskell, J. D.; Primera-Pedrozo, O. M.; Dluhy, R. A.; Zhao, Y.; Tripp, R. A. Quantitative surface-enhanced Raman spectroscopy based analysis of microRNA mixtures. *Appl. Spectrosc.* **2009**, *63*, 1107-1114.

(35) Degliangeli, F.; Kshirsagar, P.; Brunetti, V.; Pompa, P. P.; Fiammengo, R. Absolute and direct microRNA quantification using DNA-gold nanoparticle probes. *J. Am. Chem. Soc.* **2014**, *136*, 2264-2267.

(36) Longo, L.; Scorrano, S.; Vasapollo, G. RNA nucleoside recognition by phthalocyanine-based molecularly imprinted polymers. *J. Polym. Res.* **2010**, *17*, 683-687.

(37) Schildkraut, C.; Lifson, S. Dependence of the melting temperature of DNA on salt concentration. *Biopolymers* **1965**, *3*, 195-208.

(38) Xiong, X.; Wu, C.; Zhou, C.; Zhu, G.; Chen, Z.; Tan, W. Responsive DNA-Based Hydrogels and Their Applications. *Macromol. Rapid Commun.* **2013**, *34*, 1271-1283.

(39) Um, S. H.; Lee, J. B.; Park, N.; Kwon, S. Y.; Umbach, C. C.; Luo, D. Enzyme-catalysed assembly of DNA hydrogel. *Nat Mater* **2006**, *5*, 797-801.

(40) Lin, D. C.; Yurke, B.; Langrana, N. A. Mechanical properties of a reversible, DNA-crosslinked polyacrylamide hydrogel. *J Biomech Eng* **2004**, *126*, 104-110.

(41) Zhao, Y.; Zhao, X.; Tang, B.; Xu, W.; Li, J.; Hu, J.; Gu, Z. Quantum-dot-tagged bioresponsive hydrogel suspension array for multiplex label-free DNA detection. *Adv. Funct. Mater.* **2010**, *20*, 976-982.

(42) Tierney, S.; Stokke, B. T. Development of an Oligonucleotide Functionalized Hydrogel Integrated on a High Resolution Interferometric Readout Platform as a Label-Free Macromolecule Sensing Device. *Biomacromolecules* **2009**, *10*, 1619-1626.

(43) Ogiso, M.; Minoura, N.; Shinbo, T.; Shimizu, T. Detection of a specific DNA sequence by electrophoresis through a molecularly imprinted polymer. *Biomaterials* **2006**, *27*, 4177-4182.

(44) Wang, X.; Liu, X.; Wang, X. Hydrogel diffraction grating as sensor: A tool for studying volume phase transition of thermo-responsive hydrogel. *Sens. Actuators, B* **2014**, *204*, 611-616.

(45) Wang, X.; Wang, X. Aptamer-functionalized hydrogel diffraction gratings for the human thrombin detection. *Chem. Commun. (Cambridge, U. K.)* **2013**, *49*, 5957-5959.

(46) Ye, G.; Wang, X. Glucose sensing through diffraction grating of hydrogel bearing phenylboronic acid groups. *Biosens. Bioelectron.* **2010**, *26*, 772-777.

(47) Bounds, C. O.; Upadhyay, J.; Totaro, N.; Thakuri, S.; Garber, L.; Vincent, M.; Huang, Z.; Hupert, M.; Pojman, J. A. Fabrication and Characterization of Stable Hydrophilic Microfluidic Devices Prepared via the in Situ Tertiary-Amine Catalyzed Michael Addition of Multifunctional Thiols to Multifunctional Acrylates. *ACS Appl. Mater. Interfaces* **2013**, *5*, 1643-1655.

(48) Ouldridge, T. E.; Sulc, P.; Romano, F.; Doye, J. P. K.; Louis, A. A. DNA hybridization kinetics: zippering, internal displacement and sequence dependence. *Nucleic Acids Res.* **2013**, *41*, 8886-8895.

(49) Murakami, Y.; Maeda, M. DNA-Responsive Hydrogels That Can Shrink or Swell. *Biomacromolecules* **2005**, *6*, 2927-2929.

(50) Huang, X.; Brazel, C. S. On the importance and mechanisms of burst release in matrix-controlled drug delivery systems. *Journal of Controlled Release* **2001**, *73*, 121-136.

APPENDIX A: EFFECTS OF INITIATORS ON ENANTIOMER SEPARATIONS

A short study was done in the form of improved separations by changing the initiator to a compound that has some functional interactions with the template. The work described here is compared to a previous study that evaluated the enhanced performance of NOBE as an OMNiMIP as compared to the traditional imprinting approach with EGDMA and MAA using Azobisisobutyronitrile (AIBN, 17) as the initiator.[1] Of interest was the polymers imprinted with (S)-(−)-1-(1-Naphthyl)ethylamine (NEA, 20) as the initiator. Unlike many of the imprinted material in the study, the EGDMA/MAA imprinted material performed better with an α' of 2.54 and NOBE with an α' of 1.35 (Figure A.1).

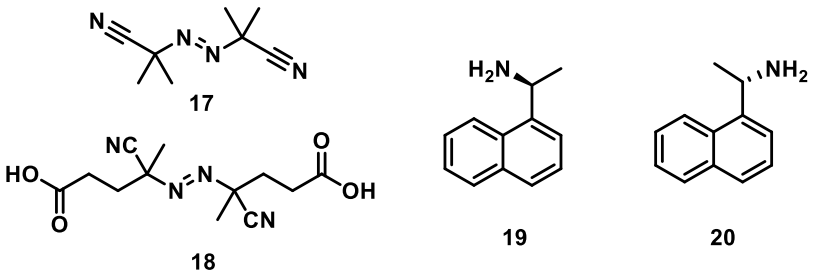

Figure A.1 Structures of AIBN 17, ACVA 18, and R- and S-NEA 19 and 20, respectively.

The new initiator of interest was 4,4′-Azobis(4-cyanovaleric acid) (ACVA, 18). This new initiator has carboxylic acid groups on each end that could provide additional functional interactions between it and the NEA template. The results are displayed in Table A.1 where both a NOBE polymer (entry 3) was made with ACVA and EGDMA (entry 4) without an additional functional monomer like MAA. As compared to the results by Martha et al., the separation factors seemed to improve for both polymers made with ACVA. The NOBE polymer had an increased α' value of 1.64 in comparison to entry 1 where the α' was 1.35. Again, the same improvement was shown for the EGDMA polymer with ACVA with an improved α' of 1.15

from 1.0 shown previously with AIBN (entry 2). The only difference between the material used here and the polymers that were previously reported was the polymer size (at 20-25µm for entry 1-2 and 25-38µm for entries 3-4) and this may have a slight effect on the separation.

Table A.1 HPLC results for NOBE and EGDMA polymers imprinted with different initiators.

Monomer	**Entry**	**Initiator**	**k'_S**	**k'_R**	**α'**
NOBE*	1	AIBN	51.9	38.5	1.35
EGDMA*	2	AIBN	2.2	2.2	1.0
NOBE	3	ACVA	8.8	5.3	1.6
EGDMA	4	ACVA	0.4	0.3	1.2

* Polymers (entries 1-3) originally reported in (Reprinted (adapted) with permission from Sibrian-Vazquez, M.; Spivak, D. A. Molecular Imprinting Made Easy. *J. Am. Chem. Soc.* **2004**, 126, 7827-7833.)[1], 20-25µm particles and 1mM analytes. Entries 3-6 were 25-38µm, analyzing 1mM analytes.

In conclusion, it was shown that the initiator can have an impact on the separation of analytes. The addition of the carboxylic acid groups on the initiator improved selectivity for both the NOBE and the EGDMA polymers. As the polymer size was different, more studies should be done to prove that there was an adequate improvement on the performance of the polymer materials.

A.1 References

(1) Sibrian-Vazquez, M.; Spivak, D. A. Molecular Imprinting Made Easy. *J. Am. Chem. Soc.* **2004**, *126*, 7827-7833.

APPENDIX B: LETTERS OF PERMISSION

Copyright Clearance Center RightsLink

Home | Account Info | Help | Live Chat

Title: Scalemic and racemic imprinting with a chiral crosslinker

Author: Britney Hebert,Danielle S. Meador,David A. Spivak

Publication: Analytica Chimica Acta

Publisher: Elsevier

Date: 26 August 2015

Logged in as:
Britney Hebert
LOGOUT

Review Order

Please review the order details and the associated terms and conditions. To edit billing or contact information please click on 'account info' at the top of this page.

Licensed content publisher	Elsevier
Licensed content publication	Analytica Chimica Acta
Licensed content title	Scalemic and racemic imprinting with a chiral crosslinker
Licensed content author	Britney Hebert,Danielle S. Meador,David A. Spivak
Licensed content date	26 August 2015
Licensed content volume number	890
Licensed content issue number	n/a
Number of pages	8
Type of Use	reuse in a thesis/dissertation
Portion	full article
Format	both print and electronic
Are you the author of this Elsevier article?	Yes
Will you be translating?	No
Title of your thesis/dissertation	MOLECULARY IMPRINTED POLYMERS FOR ENANTIOMER SEPARATIONS AND BIOMELCULAR SENSORS
Expected completion date	Aug 2016
Estimated size (number of pages)	100
Elsevier VAT number	GB 494 6272 12
Permissions price	0.00 USD
VAT/Local Sales Tax	0.00 USD / 0.00 GBP
Total	0.00 USD

THE VITA

Britney Lyn Hebert was born and raised in Houma, La. She received her Bachelor's degree in Chemistry from Nicholls State University in 2011. In August of 2011 she started the pursuit for her doctoral degree in chemistry from Louisiana State University. After joining the Spivak research group in the spring of 2012, she started investigating molecularly imprinted polymers for enantiomer separations and DNA hydrogel sensors. During her time at LSU she was awarded a GAANN fellowship and the Coates travel award. Also, Britney was an active leader in the Chemistry Graduate Student Council as a Treasurer from 2013-2014 and the treasurer of the Macromolecular Studies Graduate Student Association from 2014-2015. At the LSU summer commencement, August 5th of 2016, Britney anticipates the receipt of her degree of Doctor of Philosophy in Chemistry.